

OLLIVIER-RICCI CURVATURE FOR HYPERGRAPHS: A UNIFIED FRAMEWORK

Corinna Coupette¹, Sebastian Dalleiger^{1,2}, Bastian Rieck^{3,4}

¹Max Planck Institute for Informatics

²CISPA Helmholtz Center for Information Security

³AIDOS Lab, Institute of AI for Health, Helmholtz Munich

⁴Technical University of Munich (TUM)

ABSTRACT

Bridging geometry and topology, curvature is a powerful and expressive invariant. While the utility of curvature has been theoretically and empirically confirmed in the context of manifolds and graphs, its generalization to the emerging domain of *hypergraphs* has remained largely unexplored. On graphs, the *Ollivier-Ricci curvature* measures differences between random walks via Wasserstein distances, thus grounding a geometric concept in ideas from probability theory and optimal transport. We develop ORCHID, a flexible framework generalizing Ollivier-Ricci curvature to hypergraphs, and prove that the resulting curvatures have favorable theoretical properties. Through extensive experiments on synthetic and real-world hypergraphs from different domains, we demonstrate that ORCHID curvatures are both scalable and useful to perform a variety of hypergraph tasks in practice.

1 INTRODUCTION

Hypergraphs generalize graphs by allowing any number of nodes to participate in an edge. They enable us to faithfully represent complex relations, such as co-authorship of scientific papers, multi-lateral interactions between chemicals, or group conversations, which cannot be adequately captured by graphs. While hypergraphs are more expressive than graphs and other relational objects like simplicial complexes, they are harder to analyze both theoretically and empirically, and many concepts that have proven useful for understanding graphs have yet to be transferred to the hypergraph setting.

Curvature has established itself as a powerful characteristic of Riemannian manifolds, as it permits the description of *global properties* through *local measurements* by harmonizing ideas from geometry and topology. For graphs, *graph curvature* measures to what extent the neighborhood of an edge deviates from certain idealized model spaces, such as cliques, grids, or trees. It has proven helpful, for example, in assessing differences between real-world networks (Samal et al., 2018), identifying bottlenecks in real-world networks (Gosztolai & Arnaudon, 2021), and alleviating oversquashing in graph neural networks (Topping et al., 2022). One prominent notion of graph curvature is *Ollivier-Ricci curvature* (ORC). ORC compares random walks based at specific nodes, revealing differences in the information diffusion behavior in the graph. As the sizes of edges and edge intersections can vary in hypergraphs, there are many ways to generalize ORC to hypergraphs. While some notions of hypergraph ORC have been previously studied in isolation (e.g., Asoodeh et al., 2018; Eidi & Jost, 2020; Leal et al., 2020), a unified framework for their definition and computation is still lacking.

Contributions. We introduce ORCHID, a unified framework for Ollivier-Ricci curvature on hypergraphs. ORCHID integrates and generalizes existing approaches to hypergraph ORC. Our work is the first to identify the individual building blocks shared by all notions of hypergraph ORC, and to perform a rigorous theoretical and empirical analysis of the resulting curvature formulations. We develop hypergraph ORC notions that are aligned with our geometric intuition while still efficient to compute, and we demonstrate the utility of these notions in practice through extensive experiments.

Structure. After providing the necessary background on graphs and hypergraphs and recalling the definition of Ollivier-Ricci curvature for graphs in Section 2, we introduce ORCHID, our framework for hypergraph ORC, and analyze the theoretical properties of ORCHID curvatures in Section 3. We assess the empirical properties and practical utility of ORCHID curvatures through extensive experiments in Section 4, and discuss limitations and potential extensions of ORCHID as well as directions for future work in Section 5. Further materials are provided in Appendices A.1 to A.5.

2 PRELIMINARIES

Graphs and Hypergraphs A *simple graph* $G = (V, E)$ is a tuple containing n nodes (vertices) $V = \{v_1, \dots, v_n\}$ and m edges $E = \{e_1, \dots, e_m\}$, with $e_i \in \binom{V}{2}$ for all $i \in [m]$. Here, for a set S and a positive integer $k \leq |S|$, $\binom{S}{k}$ denotes the set of all k -element subsets of S , and for $x \in \mathbb{N}$ with $0 \notin \mathbb{N}$, $[x] = \{i \in \mathbb{N} \mid i \leq x\}$. In *multi-graphs*, edges can occur multiple times, and hence, $E = (e_1, \dots, e_m)$ is an indexed family of sets, with $e_i \in \binom{V}{2}$ for all $i \in [m]$. Generalizing simple graphs, a *simple hypergraph* $H = (V, E)$ is a tuple containing n nodes V and m hyperedges $E \subseteq \mathcal{P}(V) \setminus \emptyset$, i.e., in contrast to edges, hyperedges can have any cardinality $r \in [n]$. In a *multi-hypergraph*, $E = (e_1, \dots, e_m)$ is an indexed family of sets, with $e_i \subseteq V$ for all $i \in [m]$. We assume that all our hypergraphs are multi-hypergraphs, and we drop the prefix *hyper* from *hypergraph* and *hyperedge* where it is clear from context.

We denote the degree of node i , i.e., the number of edges containing i , by $\deg(i) = |\{e \in E \mid i \in e\}|$, write $i \sim j$ if i is adjacent to j (i.e., there exists $e \in E$ such that $\{i, j\} \subseteq e$), and use $\mathcal{N}(i)$ ($\mathcal{N}(e)$) for the neighborhood of i (e), i.e., the set of nodes adjacent to i (edges intersecting edge e). While $\deg(i) = |\mathcal{N}(i)|$ in simple graphs and $\deg(i) \geq |\mathcal{N}(i)|$ in multigraphs, these relations do not generally hold for hypergraphs. Two nodes $i \neq j$ are *connected* in H if there is a sequence of nodes $i = v_1, v_2, \dots, v_{k-1}, v_k = j$ such that $v_l \sim v_{l+1}$ for all $l \in [k]$. Every such sequence is a *path* in H , whose *length* is the cardinality of the set of edges used in the adjacency relation. We refer to the length of a shortest path connecting nodes i, j as the *distance* between them, denoted as $d(i, j)$. We assume that all (hyper)graphs are *connected*, i.e., there exists a path between all pairs of nodes. This turns H into a metric space (H, d) with *diameter* $\text{diam}(H) := \max\{d(i, j) \mid i, j \in V\}$.

(Hyper)graphs in which all nodes have the same degree k ($\deg(i) = k$ for all $i \in V$) are called *k-regular*. Three properties of hypergraphs that distinguish them from graphs give rise to additional (ir)regularities. First, *hyperedges* can vary in cardinality, and a hypergraph in which all hyperedges have the same cardinality r ($|e| = r$ for all $e \in E$) is called *r-uniform*. Second, *hyperedge intersections* can have cardinality greater than 1, and we call a hypergraph *s-intersecting* if all nonempty edge intersections have the same cardinality s ($e \cap f \neq \emptyset \Leftrightarrow |e \cap f| = s$ for all $e, f \in E$). Third, nodes can *cooccur in any number of hyperedges*; we call a hypergraph *c-cooccurrent* if each node cooccurs c times with any of its neighbors ($i \sim j \Leftrightarrow |\{e \in E \mid \{i, j\} \subseteq e\}| = c$ for all $i, j \in V$). Using this terminology, simple graphs are 2-uniform, 1-intersecting, 1-cooccurrent hypergraphs.

Given a hypergraph $H = (V, E)$, the *unweighted clique expansion* of H is $G^\circ = (V, E^\circ)$ with $E^\circ = \{\{i, j\} \mid \{i, j\} \subseteq e \text{ for some } e \in E\}$, where two nodes are adjacent in G° if and only if they are adjacent in H . The *weighted clique expansion* of H is G° endowed with a weighting function $w: E^\circ \rightarrow \mathbb{N}$, where $w(e) = |\{e \in E \mid \{i, j\} \subseteq e\}|$ for each $e \in E^\circ$, i.e., an edge $\{i, j\}$ is weighted by how often i and j cooccur in edges from H . Both of these transformations are lossy, i.e., we cannot uniquely reconstruct H from G° . The *unweighted star expansion* of H is the bipartite graph $G' = (V', E')$ with $V' = V \cup E$ and $E' = \{\{i, e\} \mid i \in V, e \in E, i \in e\}$, and we can uniquely reconstruct H from G' if we know which of its parts corresponds to the original node set of H .

Ollivier-Ricci Curvature for Graphs Ollivier-Ricci curvature (ORC) extends the notion of Ricci curvature, defined for Riemannian manifolds, to metric spaces equipped with a probability measure or, equivalently, a random walk (Ollivier, 2007; 2009). On graphs, which are metric spaces with the shortest-path distance $d(\cdot, \cdot)$, the ORC κ of a pair of nodes $\{i, j\}$ is defined as

$$\kappa(i, j) := 1 - \frac{1}{d(i, j)} W_1(\mu_i, \mu_j), \text{ and hence, } \kappa(i, j) = 1 - W_1(\mu_i, \mu_j) \text{ if } i \sim j, \quad (1)$$

where μ_i is a probability measure associated with node i that depends measurably on i and has finite first moment, and W_1 is the *Wasserstein distance* of order 1, which captures the amount of

work needed to transport the probability mass from μ_i to μ_j in an optimal coupling. The use of the shortest-path distance is necessary to ensure that ORC is also well-defined for pairs of non-adjacent nodes. This definition on edges or pairs of nodes alludes to the fact that Ricci curvature is associated to tangent vectors of a manifold. A common strategy to measure curvature at a node i is to average over the curvatures of all edges incident with i (Banerjee, 2021; Jost & Liu, 2014), i.e.,

$$\kappa(i) = \frac{1}{\deg(i)} \sum_{\{i,j\} \in E} \kappa(i,j). \quad (2)$$

A popular probability measure that easily generalizes to weighted graphs and multigraphs is

$$\mu_i^\alpha(j) := \begin{cases} \alpha & j = i \\ (1 - \alpha) \frac{1}{\deg(i)} & i \sim j \\ 0 & \text{otherwise,} \end{cases} \quad (3)$$

where α serves as a smoothing parameter (Lin et al., 2011). With this definition, stacking the probability measures yields the transition matrix of an α -lazy random walk.

3 THEORY

Having introduced the concept of hypergraphs and the definition of Ollivier-Ricci curvature (ORC) for graphs, we now develop our framework for ORC on hypergraphs, called ORCHID (Ollivier-Ricci Curvature for Hypergraphs In Data). We focus our exposition on undirected, unweighted multi-hypergraphs, but ORCHID straightforwardly generalizes to other hypergraph variants.

3.1 OLLIVIER-RICCI CURVATURES FOR HYPERGRAPHS (ORCHID CURVATURES)

As mentioned in Section 2, hypergraphs differ from graphs in that edges can have any cardinality, and consequently, edges can intersect in more than one node, and nodes can co-occur in more than one edge. When generalizing ORC as defined in Section 2 to hypergraphs, these peculiarities become relevant in two places: (1) in the generalization of the measure μ for nodes, and (2) in the generalization of the distance metric W_1 . Construing the distance metric as a function *aggregating* measures (AGG), with $\text{AGG}: V^+ \rightarrow \mathbb{R}$, we can rewrite Eq. (1) for pairs of nodes $\{i, j\}$ as

$$\kappa(i, j) := 1 - \frac{\text{AGG}(\mu_i, \mu_j)}{d(i, j)}, \quad (4)$$

which facilitates its generalization; we will also use $\kappa(e)$ for (hyper)edges as a shorthand notation for Eq. (4). When defining probability measures and AGG functions on hypergraphs, we would like to retain as much flexibility as possible while also ensuring the following conditions:

- I. *Mathematical generalization.* For graphs, AGG simplifies to the original ORC on graphs.
- II. *Permutation invariance.* $\text{AGG}(e) = \text{AGG}(\sigma(e))$ for edges e and all node index permutations σ .
- III. *Scalability.* The probability measures and AGG functions should be efficiently computable.

Beyond these properties, we would also like to have the following *interpretability* features to ascertain that a hypergraph curvature measure is a *conceptual generalization* of ORC:

- A. *Probabilistic intuition.* The probability measures assigned to nodes should correspond to a semantically sensible random walk on the hypergraph.
- B. *Optimal transport intuition.* The generalization of the distance metric (AGG) should have a semantically sensible interpretation in terms of optimal transport.
- C. *Geometric intuition.* Edges in hypercliques should have positive curvature, edges in hypergrids should have curvature zero, and edges in hypertrees should have negative curvature.

We now specify probability measures and AGG functions for which the conditions above hold.

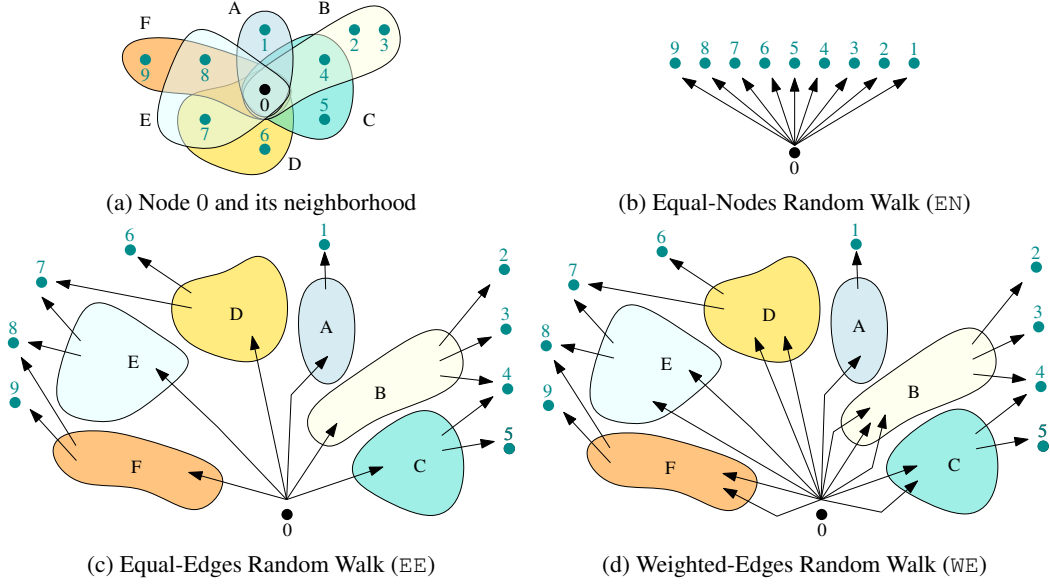


Figure 1: ORCHID’s probability measures are based on random walks, depicted for the neighborhood of a node 0. Arrows outgoing from the same node or edge are traversed with uniform probability.

Probability Measures (μ). In graphs, the most natural probability measures are induced by the α -lazy random walk given in Eq. (3): With probability α , we stay at the current node i , and with probability $(1-\alpha)/\deg(i)$, we move to one of its neighbors. There are at least three direct extensions of this formulation to hypergraphs that all retain this probabilistic intuition, thus fulfilling the requirement of Feature A. These extensions, illustrated in Fig. 1, differ only in how they distribute the $(1-\alpha)$ probability mass in Eq. (3) from node i to the nodes in i ’s neighborhood. Given a hypergraph H , for i and j with $i \sim j$, first, we could define

$$\mu_i^{\text{EN}}(j) := (1 - \alpha) \frac{1}{|\mathcal{N}(i)|}, \quad (5)$$

by which we pick a neighbor j of node i uniformly at random. We call this the *equal-nodes random walk* (EN), which is a random walk on the *unweighted clique expansion* of H . Second, we could set

$$\mu_i^{\text{EE}}(j) := (1 - \alpha) \frac{1}{\deg(i) - |\{e \ni i \mid |e| = 1\}|} \sum_{e \ni \{i,j\}} \frac{1}{|e| - 1}, \quad (6)$$

which first picks an edge $e \ni i$ with $|e| \geq 2$, then picks a node $j \in e \setminus \{i\}$, both uniformly at random. We call this the *equal-edges random walk* (EE), which is a two-step random walk on the *unweighted star expansion* of H , starting at a node $i \in V$, and non-backtracking in the second step. It underlies the curvatures studied by Asoodeh et al. (2018) and Banerjee (2021). Third, we could define

$$\mu_i^{\text{WE}}(j) := (1 - \alpha) \sum_{e \ni \{i,j\}} \frac{|e| - 1}{\sum_{f \ni i} (|f| - 1)} \frac{1}{|e| - 1} = (1 - \alpha) \frac{|\{e \in E \mid \{i,j\} \subseteq e\}|}{\sum_{f \ni i} (|f| - 1)}, \quad (7)$$

first picking an edge e incident with i with probability proportional to its cardinality, then picking a node $j \in e \setminus \{i\}$ uniformly at random. We call this the *weighted-edges random walk* (WE): a two-step random walk from a node $i \in V$ on a specific *directed weighted star expansion* of H whose second step is non-backtracking—or equivalently, a random walk on a *weighted clique expansion* of H .

Similarity Measures (AGE). In the original formulation of ORC, i.e., Eq. (1), when determining the curvature of an edge $\{i, j\}$, the Wasserstein distance W_1 is used to aggregate the probability measures of i and j . There are at least three different extensions of this aggregation scheme to hypergraphs that retain an optimal transport intuition, as required by Feature B. Leveraging that an edge $e \subseteq V$ is simply a set of nodes, the easiest extension is to leave the aggregation function

unchanged. We continue determining the curvature for pairs of nodes, and account for the edges in H only in the definition of our probability measure. In this case, we could derive a curvature for an edge e as the average over all curvatures of node pairs contained in e , i.e., we could define AGG as

$$\text{AGG}_A(e) := \frac{2}{|e|(|e|-1)} \sum_{\{i,j\} \subseteq e} W_1(\mu_i, \mu_j). \quad (8)$$

This is equivalent to computing the curvature of e based on the average over all W_1 distances of probability measures associated with nodes contained in e :

$$\kappa_A(e) := 1 - \text{AGG}_A(e) = 1 - \frac{2}{|e|(|e|-1)} \sum_{\{i,j\} \subseteq e} W_1(\mu_i, \mu_j) = \frac{2}{|e|(|e|-1)} \sum_{\{i,j\} \subseteq e} \kappa(i, j). \quad (9)$$

Intuitively, this definition assesses the mean amount of work needed to transport the probability mass from one node in e to another node in e . Alternatively, and still keeping with the intuition from optimal transport, we can define AGG as

$$\text{AGG}_B(e) := \frac{1}{|e|-1} \sum_{i \in e} W_1(\mu_i, \bar{\mu}), \quad \text{and consequently, } \kappa_B(e) := 1 - \text{AGG}_B(e), \quad (10)$$

where $\bar{\mu}$ denotes the Wasserstein barycenter of the probability measures of nodes contained in e , and the denominator generalizes the original $d(i, j)$. Asoodeh et al. (2018) use this aggregation function. Intuitively, AGG_B is proportional to the minimum amount of work needed to transport all probability mass from the probability measures of the nodes to one place, with the caveat that this place need not correspond to a node in the underlying hypergraph. Finally, we can capture the maximum amount of work needed to transport all probability mass from one node in e to another node in e as

$$\text{AGG}_M(e) := \max\{W_1(\mu_i, \mu_j) \mid \{i, j\} \subseteq e\}, \quad \text{and consequently, } \kappa_M(e) := 1 - \text{AGG}_M(e). \quad (11)$$

Independent of the choice of AGG , the curvature at a node i can be defined as the mean of all curvatures of meaningful directions containing i , i.e.,

$$\kappa^{\mathcal{N}}(i) := \frac{1}{|\mathcal{N}(i)|} \sum_{j \in \mathcal{N}(i)} \kappa(i, j), \quad (12)$$

or it can be derived as the mean of all curvatures of edges containing i , i.e.,

$$\kappa^E(i) := \frac{1}{\text{deg}(i)} \sum_{e \ni i} \kappa(e). \quad (13)$$

Finally, since H is connected, we can define the curvature of an arbitrary subset of nodes $s \subseteq V$ as

$$\kappa(s) := 1 - \frac{\text{AGG}(s)}{d(s)}, \quad (14)$$

where AGG can be any of our aggregation functions, and $d(s) := \max\{d(i, j) \mid \{i, j\} \subseteq s\}$ refers to the *extent* of the subset s . Note that for $s \in E$, $d(s) = 1$, and thus, Eq. (14) is consistent with our previous definitions of hyperedge curvatures.

3.2 PROPERTIES OF ORCHID CURVATURES

Having introduced our probability measures (μ) and aggregation functions (AGG), we now analyze their properties and the properties of the resulting curvatures. All proofs are deferred to Appendix A.1. First, we note that μ^{EN} , μ^{EE} , and μ^{WE} are equivalent for certain hypergraph classes, and all aggregation functions coincide for graphs.

Lemma 1. *For graphs and r -uniform, k -regular, c -cooccurrent hypergraphs, $\mu^{\text{EN}} = \mu^{\text{EE}} = \mu^{\text{WE}}$.*

Lemma 2. *For graphs, i.e., 2-uniform hypergraphs, we have $\text{AGG}_A(e) = \text{AGG}_B(e) = \text{AGG}_M(e)$ for all edges $e \in E$.*

Taken together, Lemma 1 and Lemma 2 imply that for graphs, ORCHID simplifies to ORC, regardless of the choice of probability measure and aggregation function. This fulfills Condition I. Moreover, *all* our aggregation functions are permutation-invariant by construction, thus satisfying Condition II. Concerning Condition III, $\kappa_{\mathbb{A}}$ and $\kappa_{\mathbb{M}}$ exhibit better scalability than $\kappa_{\mathbb{B}}$, as Wasserstein barycenters are harder to compute than individual distances (Cuturi & Doucet, 2014). Another reason to prefer $\kappa_{\mathbb{A}}$ and $\kappa_{\mathbb{M}}$ over $\kappa_{\mathbb{B}}$ is the existence of upper and lower bounds that are easy to calculate. To this end, let $d_{\min}(H) := \min\{d(u, v) \mid u \neq v \in V\}$ be the smallest nonzero distance in H , and let $\|\cdot\|_1$ refer to the L_1 norm of a vector. We then obtain the following bounds for $\kappa_{\mathbb{A}}$ and $\kappa_{\mathbb{M}}$.

Theorem 3. *For any probability measure μ and $C(e) := 2/|e|(|e|-1)$, the curvature $\kappa_{\mathbb{A}}(e)$ of an edge $e \in E$ is bounded by*

$$1 - \text{diam}(H)C(e) \sum_{\{i,j\} \subseteq e} \|\mu_i - \mu_j\|_1 \leq \kappa_{\mathbb{A}}(e) \leq 1 - d_{\min}(H)C(e) \sum_{\{i,j\} \subseteq e} \|\mu_i - \mu_j\|_1. \quad (15)$$

Theorem 4. *For any probability measure μ , the curvature $\kappa_{\mathbb{M}}(e)$ of an edge $e \in E$ is bounded by*

$$1 - \text{diam}(H) \max_{\{i,j\} \subseteq e} \|\mu_i - \mu_j\|_1 \leq \kappa_{\mathbb{M}}(e) \leq 1 - d_{\min}(H) \max_{\{i,j\} \subseteq e} \|\mu_i - \mu_j\|_1. \quad (16)$$

Directly from our definitions, we further obtain the following relationships between $\kappa_{\mathbb{A}}$, $\kappa_{\mathbb{B}}$, and $\kappa_{\mathbb{M}}$, and between ORCHID curvatures on hypergraphs and ORC on their unweighted clique expansions.

Corollary 5. *Given a hypergraph $H = (V, E)$, $\kappa_{\mathbb{M}}(e) \leq \kappa_{\mathbb{A}}(e)$ and $\kappa_{\mathbb{M}}(e) \leq \kappa_{\mathbb{B}}(e)$ for all $e \in E$.*

Corollary 6. *Given a hypergraph $H = (V, E)$ and its unweighted clique expansion $G^\circ = (V, E^\circ)$, for $\{i, j\} \in E^\circ$, the ORC $\kappa(i, j)$ in G° equals its ORCHID curvature $\kappa(i, j)$ of direction $\{i, j\} \subseteq V$ in H with μ^{EN} , and the ORC $\kappa(i)$ of $i \in V$ in G° equals its ORCHID curvature $\kappa^{\mathbb{N}}(i)$ in H with μ^{EN} .*

Corollary 6 clarifies that the equal-nodes random walk establishes the connection between ORCHID and ORC on graphs. Moreover, ORCHID curvatures capture relations between *global* properties and *local* measurements, similar to the Bonnet–Myers theorem in Riemannian geometry (Myers, 1941).

Theorem 7. *Given a subset of nodes $s \subseteq V$ and an arbitrary probability measure μ , let δ_i denote a Dirac measure at node i , and let $J(\mu_i) := W_1(\delta_i, \mu_i)$ denote the jump probability of μ_i . If (i) all curvatures based on μ are strictly positive, i.e., $\kappa(s) \geq \kappa > 0$ for all $s \subseteq V$, and (ii) $W_1(\mu_i, \mu_j) \leq \text{AGG}(s)$ for $\{i, j\} = \text{argmax}(d(s))$, then*

$$d(s) \leq \frac{J(i) + J(j)}{\kappa(s)}. \quad (17)$$

Note that condition (ii) of Theorem 7 is always satisfied by AGGM . Finally, in Appendix A.1, we generalize the concepts of cliques, grids, and trees (prototypical positively curved, flat, and negatively curved graphs) to hypergraphs, and we prove the following lemmas to ensure that ORCHID curvatures respect our geometric intuition, as required by Feature C.

Theorem 8 (Hyperclique curvature). *For an edge e in a hyperclique $H = (V, E)$ on n nodes with edges $E = \binom{V}{r}$ for some $r \leq n$, with $\alpha = 0$,*

$$\kappa(e) = 1 - \frac{1}{n-1}, \text{ i.e., } \lim_{n \rightarrow \infty} \kappa(e) = 1, \text{ independent of } r.$$

Theorem 9 (Hypergrid curvature). *For an edge e in a r -uniform, k -regular hypergrid, with $\alpha = 0$, $\kappa(e) = 0$, independent of r and k .*

Theorem 10 (Hypertree curvature). *For an edge e in a r -uniform, k -regular, 1-intersecting hypertree,*

$$\text{with } \alpha = 0, \kappa(e) = 1 - \left(\frac{3(k-1)}{k} + \frac{1}{(r-1)k} \right), \text{ i.e., } \lim_{k \rightarrow \infty} \kappa(e) = -2, \text{ independent of } r.$$

Table 1: Hypergraphs used in ORCHID experiments cover several domains and orders of magnitude. n and m are node and edge counts, n/m is the aspect ratio, c is the number of filled cells in the node-to-edge incidence matrix, c/nm is the density, and N is the number of hypergraphs in a collection.

(a) Individual Hypergraphs							
	Nodes	Edges	n	m	n/m	c	c/nm
aps-a	Authors	APS Papers	505 827	688 707	0.7345	2 480 373	0.000007
dblp	Authors	DBLP Papers	3 108 658	6 011 388	0.5171	19 411 479	0.000001
ndc-ai	Active Ingr.	NDC Drugs	7 090	131 450	0.0539	224 084	0.000240
ndc-pc	Pharm. Classes	NDC Drugs	1 263	70 101	0.0180	273 088	0.003084
(b) Hypergraph Collections							
	Nodes	Edges	Graphs	N	$(n/m)_{\max}$	$(c/nm)_{\max}$	
aps-av	Authors	APS Papers	Journals	19	4.698182	0.005216	
aps-cv	APS Cited P.	APS Citing P.	Journals	19	1.396552	0.028430	
dblp-v	Authors	DBLP Papers	(Groups of) Venues	1 193	5.599424	0.002443	
mus	Frequencies	Chords	Music Pieces	1 944	1.454545	0.375000	
stex	Tags	Questions	StackExchange Sites	355	1.233449	0.121528	
sha	Characters	Stage Groups	Shakespeare’s Plays	37	0.554054	0.304688	
syn-c	Hypergraph Configuration Models			250	0.5	0.005	
syn-r	Erdős-Rényi Random Hypergraph Models			250	0.5	0.005	
syn-s	Hypergraph Stochastic Block Models			250	0.5	0.005	

4 EXPERIMENTS

Having established in Section 3 that ORCHID curvatures have our desired theoretical properties, and finding that they strictly generalize both ORC on graphs and existing definitions of hypergraph ORC, we now seek to ascertain that they are also meaningful in practice. We ask the following questions:

Q1 Parametrization. How do our choices of α , μ , and AGG impact ORCHID curvatures?

Q2 Hypergraph exploration. How can ORCHID curvatures help us in exploring hypergraphs?

Q3 Hypergraph learning. How can ORCHID curvatures help us in hypergraph learning tasks?

To address these questions, we experiment with data from different domains, spanning several orders of magnitude. We investigate four *individual real-world hypergraphs* in which edges represent co-authorship (aps-a, dblp) and FDA-registered drugs (ndc-ai, ndc-pc), six *collections of real-world hypergraphs* in which edges represent questions on Stack Exchange Sites (stex), co-authorship by venues (aps-av, dblp-v), co-citation by venues (aps-cv), chords in music pieces (mus), and character cooccurrence on stage in Shakespeare’s plays (sha), as well as three *collections of synthetic hypergraphs* based on different generative models (syn-c, syn-r, syn-s), for a total of 4 321 hypergraphs. We summarize their basic properties in Table 1, and give more details on their statistics, semantics, and provenance in Appendix A.3. We implement ORCHID in Julia and Python. Our experiments are run on AMD EPYC 7702 CPUs with up to 256 cores. We discuss our implementation and results in more detail in Appendices A.4 and A.5, and make all our code, data, and results publicly available.¹

Q1 Parametrization. To understand how our choices of α , μ , and AGG impact ORCHID curvatures, we first compute the pairwise mutual information between ORCHID edge curvatures with 36 different parametrizations. As illustrated in Fig. 2, while changing α for the same combination of μ and AGG has similar effects across hypergraphs, there is no uniform pattern in the relationships between different combinations of μ and AGG . This underscores the fact that the various notions of ORCHID curvature are not redundant but rather emphasize distinct aspects of hypergraph structure. For a fine-grained view of the differences between parametrizations, we inspect the distributions of

¹<https://doi.org/10.5281/zenodo.7624573>

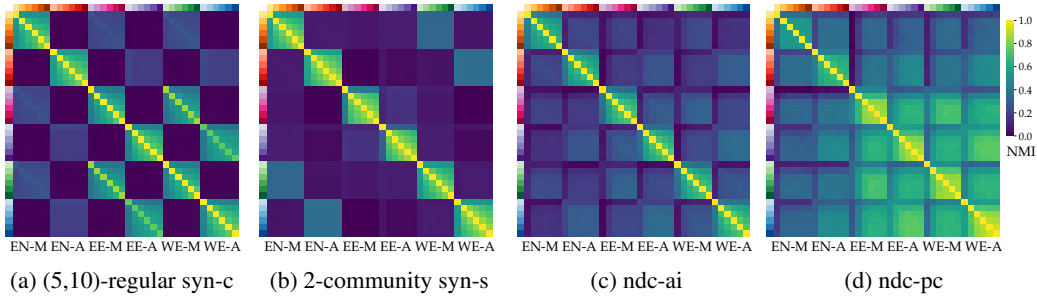


Figure 2: ORCHID curvature notions are non-redundant. We show the Min-Max-Normalized Mutual Information (NMI) between ORCHID edge curvatures with 36 different parametrizations, using probability measures μ^{EN} (EN), μ^{EE} (EE), or μ^{WE} (WE), aggregations AGG_M (M) or AGG_A (A), and $\alpha \in \{0.0, 0.1, 0.2, 0.3, 0.4, 0.5\}$ (ordered \rightarrow, \downarrow), for two synthetic and two real-world hypergraphs.

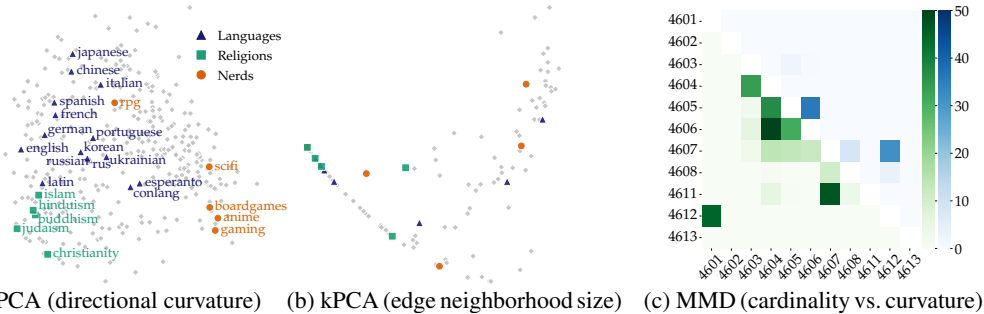


Figure 3: Curvatures carry more information than other local features. We show a 2-dimensional embedding of graphs from the stex collection based on kPCA, using an RBF kernel with curvature distributions computed using $\alpha = 0.1, \mu^{\text{WE}}$, and AGG_A (3a) or edge neighborhood size distributions (3b) as input features. We see that only curvatures yield a meaningful and discriminative grouping. Corroborating this finding, we also depict Bonferroni-adjusted p-values of testing for significant differences in feature distributions—i.e., p-values multiplied by the number h of hypothesis tests, as Bonferroni (1936) correction requires $p \leq \alpha/h$ for some desired Type I-error rate α —using MMD on distributions of edge curvatures computed with the same parameters as for (3a) (upper triangle) or edge cardinality (lower triangle), for the subset of the dblp-v collection corresponding to top conferences grouped by areas of research (3c).

our four curvature types, (i) edge curvature $\kappa(e)$, (ii) edge-averaged node curvature $\kappa^E(i)$, (iii) directional curvature $\kappa(i, j)$ for all $\{i, j\} \subseteq e \in E$, and (iv) direction-averaged node curvature $\kappa^N(i)$, for each of our 36 parametrizations. By construction, directional curvature and direction-averaged node curvature do not vary with the choice of AGG , and κ_M lower-bounds κ_A for edge curvatures and edge-averaged node curvatures. However, the differences between κ_M and κ_A vary across graphs, while consistently, the larger α , the more concentrated our curvature distributions (Appendix A.5).

Q2 Hypergraph Exploration. To explore *individual graphs*, we perform case studies on graphs from the aps-cv collection, leveraging that most nodes in these graphs also occur as edges. We scrutinize the relationships between node and edge curvatures, other local node and edge statistics, and article metadata. We observe that curvature values span a considerable range even for articles with otherwise comparable statistics, but the curvature distributions of influential papers appear to differ systematically from those of less influential papers (Appendix A.5). Exploring *graph collections*, we run kernel PCA (kPCA) (Schölkopf et al., 1997) with a radial basis function kernel (RBF kernel) and curvatures or other local features known to be powerful baselines (Cai & Wang, 2018), e.g., node degrees and neighborhood sizes, as inputs to jointly embed graphs from a collection. We statistically bootstrap the maximum mean discrepancy (MMD) (Gretton et al., 2006) to test the null hypothesis that the feature distributions of two graphs are equal. As shown in Fig. 3, ORCHID curvatures result in more interpretable embeddings and more discriminative tests than other local features.

Table 2: ORCHID curvatures lead to better clusterings than other local features. We show $WCC_{\kappa(i,j)}$ for collection clusterings computed using RBF or exp. Wasserstein kernels with edge curvatures, edge neighborhood sizes, edge-averaged node curvatures, or node neighborhood sizes as inputs.

	$RBF_{\kappa(e)}$	$W_{\kappa(e)}$	$RBF_{ \mathcal{N}(e) }$	$W_{ \mathcal{N}(e) }$	$RBF_{\kappa^E(i)}$	$W_{\kappa^E(i)}$	$RBF_{ \mathcal{N}(i) }$	$W_{ \mathcal{N}(i) }$
dblp-v	0.2151	0.1908	0.3309	0.2358	0.2273	0.0445	0.0910	0.1285
mus	0.1955	0.1758	0.2609	0.2723	0.2062	0.1606	0.2774	0.2458
stex	0.2651	0.2877	0.3018	0.2950	0.2393	0.2577	0.3067	0.2689
sha	0.5984	0.6390	0.6716	0.6597	0.5021	0.6526	0.6236	0.6641

Q3 Hypergraph Learning. To explore the utility of curvatures for learning on *individual hypergraphs*, we perform spectral clustering using either curvatures or other local node features. To evaluate the resulting node clusterings, we leverage that *nodes* in the aps-cv collection correspond to APS papers, for which we consistently know the titles. Hence, even in the absence of a meaningful ground truth, we can still check the sensibility of a clustering by statistically analyzing the titles grouped together using tools from natural language processing. We find that node clusterings based on curvatures correspond to thematically more coherent groupings (Appendix A.5). For learning on *hypergraph collections*, we spectrally cluster the collection using RBF or exponential Wasserstein kernel matrices, $\exp(-\gamma W(\mu_x, \mu_y))$, on node and edge curvatures or other local features (Plaen et al., 2020). Lacking ground-truth labels, we evaluate the clustering quality in an *unsupervised* manner, using what we call the *Wasserstein Clustering Coefficient* (WCC). This measure compares averaged *intra*-cluster Wasserstein distances to averaged *inter*-cluster Wasserstein distances, such that a *lower* WCC corresponds to a higher-quality clustering. Given c clusters $\mathcal{X} = \{X_1, \dots, X_c\}$ of hypergraphs H represented by their feature distributions $\vec{\chi}_H$, we define

$$WCC(\mathcal{X}) := \frac{\sum_{X \in \mathcal{X}} \omega(X)}{1 + \sum_{X \neq Y \in \mathcal{X}} \omega(X, Y)}, \text{ with } \begin{cases} \omega(X) := \binom{|X|}{2}^{-1} \sum_{x \neq y \in X} W(\vec{\chi}_x, \vec{\chi}_y), \\ \omega(X, Y) := (|X||Y|)^{-1} \sum_{x, y \in X \times Y} W(\vec{\chi}_x, \vec{\chi}_y). \end{cases}$$

As illustrated in Table 2, when evaluated using WCC with directional curvature distributions as $\vec{\chi}$, i.e., $WCC_{\kappa(i,j)}$, ORCHID curvatures consistently yield better clusterings than other local features.

5 DISCUSSION AND CONCLUSION

We introduced ORCHID, the first unified framework for Ollivier-Ricci curvature on hypergraphs that integrates and generalizes existing approaches to hypergraph ORC. ORCHID disentangles the common building blocks of all notions of hypergraph ORC, yielding curvature notions that are provably aligned with our geometric intuition. We performed a rigorous theoretical and empirical analysis of ORCHID curvatures, demonstrating their practical utility and scalability through extensive experiments, covering both *hypergraph exploration* and *hypergraph learning*. While our work paves the way toward future work seeking to leverage the power of Ollivier-Ricci curvature for hypergraphs in hypergraph learning algorithms, it still has some limitations to be addressed. First, ORC on graphs is defined for *any* probability measure, but we only consider measures corresponding to a single step of a random walk. Future work could thus harness higher-order random walks or alternative probability measures, and consider analyzing relationships between such probability measures and other structural hypergraph properties. Second, hyperedge intersections can vary in cardinality, but this variation is not currently reflected in our probability measures. One could thus integrate ORCHID with the s -walk framework proposed by Aksoy et al. (2020), or define persistent ORCHID curvatures based on hypergraph filtrations, extending work on persistent ORC for graphs (Wee & Xia, 2021b). Third, like the original ORC, ORCHID curvatures are static, but many hypergraphs are inherently dynamic, suggesting a need to develop dynamic curvature notions. Fourth, despite its comprehensive scope, our study only scratches the surface regarding the theoretical and empirical analysis of ORCHID curvatures, and we believe that there are many more connections between ORCHID curvatures and other hypergraph descriptors to be uncovered, and many additional use cases to be explored. For instance, ORCHID generalizes ORC, but not Forman-Ricci curvature (FRC), and we believe that a framework for FRC could help uncover new relations between combinatorial curvature notions and hypergraph structure. Finally, we imagine that incorporating hypergraph curvature into models as an additional inductive bias could prove useful in hypergraph learning more broadly.

ETHICS STATEMENT

Our main contribution is ORCHID, a unified mathematical framework yielding theoretically sound hypergraph descriptors that are also practically useful for hypergraph exploration and hypergraph learning. As such, ORCHID comes with the caveats applicable to hypergraph exploration and hypergraph learning methods more generally. Most importantly, it should be used with caution on data related to people, and its results should not be decontextualized. We adhered to these principles in our experiments, and selected our datasets accordingly.

REPRODUCIBILITY STATEMENT

To facilitate reproducibility, we provide more details on our data, implementation, and results in more detail in Appendices A.3 to A.5, and make all our code, data, and results publicly available at <https://doi.org/10.5281/zenodo.7624573>.

REFERENCES

- Tomoya Akamatsu. A new transport distance and its associated ricci curvature of hypergraphs. *Analysis and Geometry in Metric Spaces*, 10(1):90–108, 2022.
- Sinan G. Aksoy, Cliff Joslyn, Carlos Ortiz Marrero, Brenda Praggastis, and Emilie Purvine. Hyper-network science via high-order hypergraph walks. *EPJ Data Science*, 9(1):16, 2020.
- Ilya Amburg, Nate Veldt, and Austin Benson. Clustering in graphs and hypergraphs with categorical edge labels. In *Proceedings of the Web Conference 2020*, pp. 706–717, 2020.
- Shahab Asoodeh, Tingran Gao, and James Evans. Curvature of hypergraphs via multi-marginal optimal transport. In *IEEE Conference on Decision and Control (CDC)*, pp. 1180–1185, 2018.
- Lu Bai, Peng Ren, and Edwin R Hancock. A hypergraph kernel from isomorphism tests. In *International Conference on Pattern Recognition (ICPR)*, pp. 3880–3885, 2014.
- Dominique Bakry and Michel Émery. Diffusions hypercontractives. *Séminaire de probabilités de Strasbourg*, 19:177–206, 1985.
- Anirban Banerjee. On the spectrum of hypergraphs. *Linear Algebra and its Applications*, 614: 82–110, 2021.
- F Bauer, F Chung, Y Lin, and Y Liu. Curvature aspects of graphs. *Proceedings of the American Mathematical Society*, 145(5):2033–2042, 2017.
- Isabelle Bloch and Alain Bretto. Mathematical morphology on hypergraphs, application to similarity and positive kernel. *Computer Vision and Image Understanding*, 117(4):342–354, 2013.
- Carlo Bonferroni. Teoria statistica delle classi e calcolo delle probabilita. *Pubblicazioni del R Istituto Superiore di Scienze Economiche e Commerciali di Firenze*, 8:3–62, 1936.
- David P. Bourne, David Cushing, Shiping Liu, Florentin Münch, and Norbert Peyerimhoff. Ollivier-Ricci idleness functions of graphs. *SIAM Journal on Discrete Mathematics*, 32(2):1408–1424, 2018.
- Chen Cai and Yusu Wang. A simple yet effective baseline for non-attributed graph classification. *arXiv:1811.03508*, 2018.
- Corinna Coupette, Jilles Vreeken, and Bastian Rieck. All the world’s a (hyper)graph: A data drama. *arXiv:2206.08225*, 2022.
- Mihai Cucuringu, Peter Davies, Aldo Glielmo, and Hemant Tyagi. SPONGE: A generalized eigenproblem for clustering signed networks. In Kamalika Chaudhuri and Masashi Sugiyama (eds.), *International Conference on Artificial Intelligence and Statistics (AISTATS)*, pp. 1088–1098, 2019.

- Marco Cuturi and Arnaud Doucet. Fast computation of wasserstein barycenters. In Eric P. Xing and Tony Jebara (eds.), *International Conference on Machine Learning (ICML)*, volume 32, pp. 685–693, 2014.
- Manh Tuan Do, Se-eun Yoon, Bryan Hooi, and Kijung Shin. Structural patterns and generative models of real-world hypergraphs. In *Proceedings of the 26th ACM SIGKDD International Conference on Knowledge Discovery & Data Mining (KDD)*, pp. 176–186, 2020.
- Marzieh Eidi and Jürgen Jost. Ollivier–Ricci curvature of directed hypergraphs. *Scientific Reports*, 10(1):1–14, 2020.
- Robin Forman. Bochner’s method for cell complexes and combinatorial Ricci curvature. *Discrete and Computational Geometry*, 29(3):323–374, 2003.
- Tingran Gao, Shahab Asoodeh, Yi Huang, and James Evans. Wasserstein soft label propagation on hypergraphs: Algorithm and generalization error bounds. In *AAAI Conference on Artificial Intelligence*, pp. 3630–3637, 2019.
- Alison L. Gibbs and Francis Edward Su. On choosing and bounding probability metrics. *International Statistical Review*, 70(3):419–435, 2002.
- Adam Gosztoi and Alexis Arnaudon. Unfolding the multiscale structure of networks with dynamical Ollivier–Ricci curvature. *Nature Communications*, 12(1):4561, 2021. doi: 10.1038/s41467-021-24884-1.
- Arthur Gretton, Karsten Borgwardt, Malte Rasch, Bernhard Schölkopf, and Alex Smola. A kernel method for the two-sample-problem. *Advances in Neural Information Processing Systems*, 19, 2006.
- Jing Huang and Jie Yang. UniGNN: a unified framework for graph and hypergraph neural networks. In *Proceedings of the 30th International Joint Conference on Artificial Intelligence (IJCAI)*, pp. 2563–2569, 2021.
- Masahiro Ikeda, Yu Kitabeppu, Yuuki Takai, and Takato Uehara. Coarse Ricci curvature of hypergraphs and its generalization. *arXiv:2102.00698*, 2021.
- Jürgen Jost and Shiping Liu. Ollivier’s Ricci curvature, local clustering and curvature-dimension inequalities on graphs. *Discrete & Computational Geometry*, 51(2):300–322, 2014.
- Mark Kempton, Gabor Lippner, and Florentin Münch. Large scale Ricci curvature on graphs. *Calculus of Variations and Partial Differential Equations*, 59(5):1–17, 2020.
- Wilmer Leal, Marzieh Eidi, and Jürgen Jost. Curvature-based analysis of directed hypernetworks. *Complex Networks*, pp. 10–12, 2019.
- Wilmer Leal, Marzieh Eidi, and Jürgen Jost. Ricci curvature of random and empirical directed hypernetworks. *Applied Network Science*, 5(1):65, 2020.
- Wilmer Leal, Guillermo Restrepo, Peter F. Stadler, and Jürgen Jost. Forman–Ricci curvature for hypergraphs. *Advances in Complex Systems*, 24(1):2150003:1–2150003:24, 2021.
- Geon Lee and Kijung Shin. THyMe+: Temporal hypergraph motifs and fast algorithms for exact counting. In *IEEE International Conference on Data Mining (ICDM)*, pp. 310–319, 2021.
- Geon Lee, Jihoon Ko, and Kijung Shin. Hypergraph motifs: concepts, algorithms, and discoveries. *Proceedings of the VLDB Endowment*, 13(12):2256–2269, 2020.
- Yong Lin, Linyuan Lu, and Shing-Tung Yau. Ricci curvature of graphs. *Tohoku Mathematical Journal, Second Series*, 63(4):605–627, 2011.
- Shiping Liu, Florentin Münch, Norbert Peyerimhoff, and Christian Rose. Distance bounds for graphs with some negative Bakry–Émery curvature. *Analysis and Geometry in Metric Spaces*, 7(1):1–14, 2019.

- Peter Macgregor and He Sun. Finding bipartite components in hypergraphs. *Advances in Neural Information Processing Systems*, 34, 2021.
- Alessio Martino and Antonello Rizzi. (Hyper)graph kernels over simplicial complexes. *Entropy*, 22(10):1155, 2020.
- Florentin Münch and Christian Rose. Spectrally positive Bakry-Émery Ricci curvature on graphs. *Journal de Mathématiques Pures et Appliquées*, 143:334–344, 2020.
- Kevin A. Murgas, Emil Saucan, and Romeil Sandhu. Hypergraph geometry reflects higher-order dynamics in protein interaction networks. *Scientific Reports*, 12(1):20879, 2022.
- Sumner Byron Myers. Riemannian manifolds with positive mean curvature. *Duke Mathematical Journal*, 8(2):401–404, 1941.
- Yann Ollivier. Ricci curvature of metric spaces. *Comptes Rendus Mathématique*, 345(11):643–646, 2007.
- Yann Ollivier. Ricci curvature of markov chains on metric spaces. *Journal of Functional Analysis*, 256(3):810–864, 2009.
- Henri De Plaen, Michael Fanuel, and Johan A. K. Suykens. Wasserstein exponential kernels. *IEEE International Joint Conference on Neural Networks (IJCNN)*, 2020.
- Indrava Roy, Sudharsan Vijayaraghavan, Sarath Jyotsna Ramaia, and Areejit Samal. Forman-Ricci curvature and persistent homology of unweighted complex networks. *Chaos, Solitons & Fractals*, 140:110260, 2020.
- Areejit Samal, RP Sreejith, Jiao Gu, Shiping Liu, Emil Saucan, and Jürgen Jost. Comparative analysis of two discretizations of Ricci curvature for complex networks. *Scientific Reports*, 8(1): 1–16, 2018.
- Emil Saucan and Melanie Weber. Forman’s Ricci curvature - From networks to hypernetworks. In Luca Maria Aiello, Chantal Cherifi, Hocine Cherifi, Renaud Lambiotte, Pietro Lió, and Luis M. Rocha (eds.), *International Conference on Complex Networks and their Applications*, volume 812, pp. 706–717, 2018.
- Bernhard Schölkopf, Alexander Smola, and Klaus-Robert Müller. Kernel principal component analysis. *Artificial Neural Networks (ICANN)*, pp. 583–588, 1997.
- Jake Topping, Francesco Di Giovanni, Benjamin Paul Chamberlain, Xiaowen Dong, and Michael M. Bronstein. Understanding over-squashing and bottlenecks on graphs via curvature. In *International Conference on Learning Representations (ICLR)*, 2022.
- Nate Veldt, Anthony Wirth, and David F. Gleich. Parameterized correlation clustering in hypergraphs and bipartite graphs. In *Proceedings of the 26th ACM SIGKDD International Conference on Knowledge Discovery & Data Mining (KDD)*, pp. 1868–1876, 2020.
- Gabriel Wachman and Roni Khardon. Learning from interpretations: a rooted kernel for ordered hypergraphs. In *International Conference on Machine Learning (ICML)*, pp. 943–950, 2007.
- Melanie Weber, Emil Saucan, and Jürgen Jost. Characterizing complex networks with Forman-Ricci curvature and associated geometric flows. *Journal of Complex Networks*, 5(4):527–550, 2017. doi: 10.1093/comnet/cnw030.
- Junjie Wee and Kelin Xia. Forman persistent Ricci curvature (FPRC)-based machine learning models for protein-ligand binding affinity prediction. *Briefings in Bioinformatics*, 22(6), 2021a.
- Junjie Wee and Kelin Xia. Ollivier persistent Ricci curvature-based machine learning for the protein-ligand binding affinity prediction. *Journal of Chemical Information and Modeling*, 61(4):1617–1626, 2021b.
- Yasharth Yadav, Areejit Samal, and Emil Saucan. A poset-based approach to curvature of hypergraphs. *Symmetry*, 14(2):420, 2022.
- Dengyong Zhou, Jiayuan Huang, and Bernhard Schölkopf. Learning with hypergraphs: Clustering, classification, and embedding. *Advances in Neural Information Processing Systems*, 19, 2006.

A APPENDIX

In this Appendix, we include the following materials.

A.1 Deferred Proofs.

All proofs for Section 3, along with supporting definitions, lemmas and corollaries.

A.2 Related Work.

Discussion of related work treating hypergraph curvatures, graph curvatures, or hypergraph analysis.

A.3 Dataset Details.

Further information on the provenance, semantics, and statistics of our datasets.

A.4 Implementation Details.

Details on our implementation, including proofs showing the correctness of performance shortcuts.

A.5 Further Results.

Display and discussion of results not included in the main paper.

A.1 DEFERRED PROOFS

Lemma 1. *For graphs and r -uniform, k -regular, c -cooccurrent hypergraphs, $\mu^{\text{EN}} = \mu^{\text{EE}} = \mu^{\text{WE}}$.*

Proof. For notational simplicity, w.l.o.g., we assume that $\alpha = 0$. In an r -uniform, k -regular, c -cooccurrent hypergraph $H = (V, E)$, each node i has degree k and $\frac{(r-1)k}{c}$ neighbors, and each edge has cardinality r . Hence, for nodes $i, j \in V$ with $i \sim j$,

$$\begin{aligned} \mu_i^{\text{EN}}(j) &= \frac{1}{|\mathcal{N}(i)|} = \frac{c}{(r-1)k} = \frac{1}{k} \cdot c \cdot \frac{1}{r-1} = \frac{1}{\deg(i)} \sum_{e \ni i, j} \frac{1}{|e|-1} = \mu_i^{\text{EE}}(j) \\ &= \frac{c}{k(r-1)} = \frac{|\{e \in E \mid \{i, j\} \subseteq e\}|}{\sum_{f \ni i} (|f|-1)} = \mu_i^{\text{WE}}(j). \end{aligned}$$

Graphs are 2-uniform and 1-cooccurrent (but not generally regular), and hence, $|\mathcal{N}(i)| = \deg(i)$. Using this to simplify the probability measure expressions, the claim follows. \square

Lemma 2. *For graphs, i.e., 2-uniform hypergraphs, we have $\text{AGG}_{\text{A}}(e) = \text{AGG}_{\text{B}}(e) = \text{AGG}_{\text{M}}(e)$ for all edges $e \in E$.*

Proof. Given probability distributions $\mu_1, \mu_2, \dots, \mu_n$, their Wasserstein barycenter is defined as the distribution $\bar{\mu}$ that minimizes $f(\bar{\mu}) := \frac{1}{n} \sum_{i=1}^n W_1(\bar{\mu}, \mu_i)$. Since $|e| = 2$, we minimize $W_1(\bar{\mu}, \mu_1) + W_1(\bar{\mu}, \mu_2)$. The Wasserstein distance is a metric, so it satisfies the triangle inequality. Thus, $W_1(\mu_1, \mu_2) \leq W_1(\bar{\mu}, \mu_1) + W_1(\bar{\mu}, \mu_2)$ for all choices of $\bar{\mu}$. Hence, f is minimized by either μ_1 or μ_2 . Evaluating both cases yields $\text{AGG}_{\text{A}}(e) = \text{AGG}_{\text{B}}(e)$, and observing that $\text{AGG}_{\text{M}}(e) = W_1(\mu_i, \mu_j)$ for $e = \{i, j\}$ by definition, the claim follows. \square

Theorem 3. *For any probability measure μ and $C(e) := 2/|e|(|e|-1)$, the curvature $\kappa_{\text{A}}(e)$ of an edge $e \in E$ is bounded by*

$$1 - \text{diam}(H)C(e) \sum_{\{i, j\} \subseteq e} \|\mu_i - \mu_j\|_1 \leq \kappa_{\text{A}}(e) \leq 1 - d_{\min}(H)C(e) \sum_{\{i, j\} \subseteq e} \|\mu_i - \mu_j\|_1. \quad (15)$$

Proof. We bound each of the summands in the curvature calculation. Given probability measures μ_i, μ_j , a result by Gibbs & Su (2002, Theorem 4) states that

$$d_{\min}(H) d_{\text{TV}}(\mu_i, \mu_j) \leq W_1(\mu_i, \mu_j) \leq \text{diam}(H) d_{\text{TV}}(\mu_i, \mu_j), \quad (18)$$

where d_{TV} refers to the *total variation distance*. The intuition behind this bound is that the total variation distance represents a specific type of transport plan between the two probability measures; the factors arising from the minimum (maximum) distance in a space indicate the minimum (maximum) distance that realizes this transport plan. Since all our measures are defined over a finite space, we have $d_{\text{TV}}(\mu_i, \mu_j) = 1/2 \|\mu_i - \mu_j\|_1$. The claim follows by considering that pairwise distances are being *subtracted* to calculate our curvature measure. \square

Theorem 4. For any probability measure μ , the curvature $\kappa_M(e)$ of an edge $e \in E$ is bounded by

$$1 - \text{diam}(H) \max_{\{i,j\} \subseteq e} \|\mu_i - \mu_j\|_1 \leq \kappa_M(e) \leq 1 - d_{\min}(H) \max_{\{i,j\} \subseteq e} \|\mu_i - \mu_j\|_1. \quad (16)$$

Proof. For AGG_M , Eq. (18) applies for a single pairwise distance only. We thus only obtain a single bound based on the maximum total variation distance between two probability measures. \square

Theorem 7. Given a subset of nodes $s \subseteq V$ and an arbitrary probability measure μ , let δ_i denote a Dirac measure at node i , and let $J(\mu_i) := W_1(\delta_i, \mu_i)$ denote the jump probability of μ_i . If (i) all curvatures based on μ are strictly positive, i.e., $\kappa(s) \geq \kappa > 0$ for all $s \subseteq V$, and (ii) $W_1(\mu_i, \mu_j) \leq \text{AGG}(s)$ for $\{i, j\} = \text{argmax}(d(s))$, then

$$d(s) \leq \frac{J(i) + J(j)}{\kappa(s)}. \quad (17)$$

Proof. Let $\{i, j\} = \text{argmax}(d(s))$ as required in the theorem. We then have following chain of (in)equalities:

$$d(s) = d(i, j) = W_1(\delta_i, \delta_j) \leq W_1(\delta_i, \mu_i) + W_1(\mu_i, \mu_j) + W_1(\mu_j, \delta_j). \quad (19)$$

Rearranging Eq. (14), we have $(1 - \kappa(s)) d(s) = \text{AGG}(s)$. According to our assumptions, $W_1(\mu_i, \mu_j) \leq \text{AGG}(s) = (1 - \kappa(s)) d(i, j)$. Inserting this into Eq. (19) yields

$$d(i, j) \leq J(\mu_i) + J(\mu_j) + (1 - \kappa(s)) d(i, j) \quad (20)$$

$$\Leftrightarrow d(i, j) - (1 - \kappa(s)) d(i, j) \leq J(\mu_i) + J(\mu_j) \quad (21)$$

$$\Leftrightarrow d(i, j) \leq \frac{J(i) + J(j)}{\kappa(s)}, \quad (22)$$

where the last step is only valid since $\kappa(s) \geq \kappa > 0$ by assumption. \square

Definition 11 (Hypercliques, hypergrids, hypertrees). A simple, connected hypergraph $H = (V, E)$ is

- a hyperclique if $E = \binom{V}{r}$ for some $r \leq |V|$,
- a hypergrid if H is an r -uniform hypergraph for which there exists a lattice $L = (V, E_L)$ s.t. $E = \{e \in \binom{V}{r} \mid e \text{ corresponds to a path of length } r \text{ in } L\}$, and
- a hypertree if there exists a tree $T = (V, E_T)$ s.t. each edge $e \in E_T$ induces a subtree in T .

Corollary 12. Cliques are hypercliques, grids are hypergrids, and trees are hypertrees.

Corollary 13. If $H = (V, E)$ is a hyperclique, a hypergrid, or an r -uniform, k -regular, 1-intersecting hypertree, for $i, j \in V$, the sets $S_i = \{e \in E \mid i \in e\}$ and $S_j = \{e \in E \mid j \in e\}$ are isomorphic, i.e., there exists $\varphi : \mathcal{N}(i) \cup \{i\} \rightarrow \mathcal{N}(j) \cup \{j\}$ such that $\{\{\varphi(x) \mid x \in e\} \mid e \in S_i\} = S_j$.

For hypercliques, hypergrids, and hypertrees with certain regularities, $\text{AGG}_A(e)$ and $\text{AGG}_M(e)$ are constants.

Lemma 14 (Hypercliques, hypergrids, hypertrees). If $H = (V, E)$ is a hyperclique, a hypergrid, or an r -uniform, k -regular, 1-intersecting hypertree, we have $\text{AGG}_A(e) = \text{AGG}_M(e) = W_1(\mu_i, \mu_j) = w$ for $w \in \mathbb{R}$, $e \in E$, and $i, j \in V$ with $i \sim j$.

Proof. By Corollary 13, we have $w := W_1(\mu_i, \mu_j) = W_1(\mu_p, \mu_q)$ for $i, j, p, q \in V$ with $i \sim j$ and $p \sim q$. Hence $\text{AGG}_M(e) = w$, and $\text{AGG}_A(e) = \frac{2}{|e|(|e|-1)} \sum_{\{i,j\} \subseteq e} W_1(\mu_i, \mu_j) = \frac{2}{|e|(|e|-1)} \frac{|e|(|e|-1)}{2} w = w$, for $e \in E$. \square

Corollary 15. If $H = (V, E)$ is a hyperclique, a hypergrid, or an r -uniform, k -regular, 1-intersecting hypertree, $\text{AGG}_A(e) = \text{AGG}_M(e)$.

Using Lemma 14, we now prove that under AGG_A and AGG_M , hypercliques are positively curved, hypergrids are flat, and hypertrees are negatively curved, as desired.

Theorem 8 (Hyperclique curvature). *For an edge e in a hyperclique $H = (V, E)$ on n nodes with edges $E = \binom{V}{r}$ for some $r \leq n$, with $\alpha = 0$,*

$$\kappa(e) = 1 - \frac{1}{n-1}, \text{ i.e., } \lim_{n \rightarrow \infty} \kappa(e) = 1, \text{ independent of } r.$$

Proof. A hyperclique is r -uniform, $(n-1)$ -regular, and $(r-2)$ -cooccurrent, so $\mu_i^{\text{EN}} = \mu_i^{\text{EE}} = \mu_i^{\text{WE}}$ for each node $i \in V$ by Lemma 1. Thus, considering μ_i^{EN} , each node $i \in V$ has $n-1$ neighbors to which it distributes its probability mass equally, and we have $W_1(\mu_i, \mu_j) = \frac{1}{n-1}$ for $i, j \in V$ with $i \sim j$. The claim now follows from Lemma 14. \square

Theorem 9 (Hypergrid curvature). *For an edge e in a r -uniform, k -regular hypergrid, with $\alpha = 0$, $\kappa(e) = 0$, independent of r and k .*

Proof. By Corollary 13, the sets $S_i = \{e \in E \mid i \in e\}$ and $S_j = \{e \in E \mid j \in e\}$ are isomorphic, and due to the symmetries in the hypergrid, the isomorphism $\varphi: \mathcal{N}(i) \cup \{i\} \rightarrow \mathcal{N}(j) \cup \{j\}$ minimizing the cost $\sum_{x \in \mathcal{N}(i) \cup \{i\}} d(x, \varphi(x))$ corresponds to the coupling minimizing $W_1(\mu_i, \mu_j)$. The cost of φ equals the minimum cost of an isomorphism in H 's underlying lattice L between the inclusive $(r-1)$ -hop neighborhoods of two nodes adjacent in L , which is $|\mathcal{N}(i) \cup \{i\}|$. Hence, $W_1(\mu_i, \mu_j) = \frac{|\mathcal{N}(i) \cup \{i\}|}{|\mathcal{N}(i) \cup \{i\}|} = 1$ for $i, j \in V$ with $i \sim j$ and all choices of μ , and the claim then follows from Lemma 14. \square

Theorem 10 (Hypertree curvature). *For an edge e in a r -uniform, k -regular, 1-intersecting hypertree,*

$$\text{with } \alpha = 0, \kappa(e) = 1 - \left(\frac{3(k-1)}{k} + \frac{1}{(r-1)k} \right), \text{ i.e., } \lim_{k \rightarrow \infty} \kappa(e) = -2, \text{ independent of } r.$$

Proof. An r -uniform, k -regular, 1-intersecting hypertree is 1-cooccurrent, so we have $\mu_i^{\text{EN}} = \mu_i^{\text{EE}} = \mu_i^{\text{WE}}$ for each node $i \in V$ by Lemma 1. Each node $i \in V$ has $(r-1)k$ neighbors, such that μ_i^{EN} distributes a fraction $\frac{1}{(r-1)k}$ of the probability mass to each of i 's neighbors. Nodes $i, j \in V$ with $i \sim j$ share $(r-2)$ neighbors (those in the unique edge e satisfying $\{i, j\} \subseteq e$), and the probability mass allocated by μ_i to j can be matched with the probability mass allocated by μ_j to i at cost 1. Because H is a hypertree, the remaining probability mass, $(r-1)(k-1)/((r-1)k) = (k-1)/k$, needs to be transported from the neighborhood of i to the neighborhood of j at cost 3. Hence,

$$W_1(\mu_i, \mu_j) = 1 \cdot \frac{1}{(r-1)k} + 3 \cdot \frac{k-1}{k}$$

for $i, j \in V$ with $i \sim j$. Again, the claim follows from Lemma 14. \square

A.2 RELATED WORK

Hypergraph Curvature Most closely related to our work is the literature on hypergraph curvatures. Much of this literature focuses on defining notions of ORC and Forman-Ricci Curvature (FRC) specifically for *directed* hypergraphs and studying some of their mathematical and empirical properties (e.g., Leal et al., 2019; 2020; 2021; Saucan & Weber, 2018). Notably, the directed hypergraph ORC introduced by Eidi & Jost (2020) is an instantiation of our framework with μ^{EE} and AGG_A . Curvature notions for *undirected* hypergraphs are comparatively less explored, and especially the literature generalizing ORC is almost entirely theoretical. The generalization of ORC proposed by Asoodeh et al. (2018) and the equivalent measure used by Banerjee (2021) are instantiations of our framework using μ^{EE} and AGG_B . Akamatsu (2022) propose (α, h) -ORC using cost functions based on structured optimal transport, and Ikeda et al. (2021) define λ -coarse Ricci curvature using a λ -nonlinear Kantorovich difference based on a submodular hypergraph Laplacian as a generalization of ORC as introduced by Lin et al. (2011). Both of these works define curvature exclusively for pairs of nodes, rather than for hyperedges. Beyond ORC, Yadav et al. (2022) study FRC for undirected hypergraphs defined via poset representations, and Murgas et al. (2022) explore hypergraphs constructed from protein-protein interactions using a different notion of FRC based on the Hodge Laplacian. To the best of our knowledge, with ORCHID, we are the first to introduce a flexible framework generalizing ORC to hypergraphs, and to demonstrate the utility of hypergraph ORC in practice.

Graph Curvature. Beyond the Ollivier-Ricci concepts, there are also curvature concepts based on the contractivity of operators (Bakry & Émery, 1985), which could be considered a “spiritual precursor” to Ollivier’s work. This perspective has been used to provide a predominantly *spectral perspective* on curvature (Liu et al., 2019; Münch & Rose, 2020), whereas ORC can foremost be seen as a *probabilistic concept*. Recently, Kempton et al. (2020) defined a hybrid between Ollivier and Bakry-Émery curvature on graphs. A more combinatorial perspective is assumed by FRC, which is motivated by defining equivalent formulations of curvature on structured spaces, such as CW complexes or simplicial complexes. Originally described by Forman (2003), FRC has since been improved in the context of explaining the learning behavior of graph neural networks (Topping et al., 2022), with other recent work focusing on fusing it with topological graph properties (Roy et al., 2020). ORC was first developed for general Markov chains (Ollivier, 2007; 2009), but has quickly been adopted to characterize graphs (Jost & Liu, 2014) and networks (Weber et al., 2017). With numerous follow-up publications elucidating the relationship between structural properties of a graph and ORC (Bauer et al., 2017; Samal et al., 2018), the initial concept has also been substantially updated (Bourne et al., 2018; Lin et al., 2011). As an emerging research direction, we identified the combination of ORC (and FRC) with concepts from computational topology, leading to an inherent multi-scale perspective on data. This has led to promising results for treating biomedical graph data (Wee & Xia, 2021a;b).

Hypergraph Learning. Work tackling certain hypergraph learning tasks such as hypergraph clustering (Amburg et al., 2020; Veldt et al., 2020) has existed for many years (Wachman & Khardon, 2007; Zhou et al., 2006). Some approaches make use of intrinsic structural properties of hypergraphs, leading to hypergraph neural network architectures (Huang & Yang, 2021) and message passing formulations (Gao et al., 2019), whereas others focus on developing similarity measures, i.e., *kernels* (Bai et al., 2014; Bloch & Bretto, 2013; Martino & Rizzi, 2020). Methods from the rich literature on *graph* kernels can also be employed to address hypergraph learning tasks, namely, by transforming the hypergraph into a graph, but most popular transformations are lossy and may drastically increase the size of the object under study, such that the practicality and utility of this approach is unclear.

Hypergraph Mining and Analysis. In recent years, there has been a renewed interest in hypergraph mining and analysis. Notably, there is work developing new hypergraph descriptors (Aksoy et al., 2020), extending motif discovery to hypergraphs (Lee & Shin, 2021; Lee et al., 2020), solving classic graph mining tasks in the hypergraph setting (Macgregor & Sun, 2021), or identifying patterns in real-world hypergraphs (Do et al., 2020). However, to the best of our knowledge, none of this work draws on curvature concepts to solve the mining and analysis tasks of interest.

A.3 DATASET DETAILS

At a high level, our workflow to produce and work with the datasets used in our experiments (Section 4) was as follows:

1. Obtain raw data in a variety of different formats, e.g., CSV, JSON, or XML.
2. Transform the raw data into a hypergraph CSV that retains as much of the raw data semantics as possible. This CSV is guaranteed to contain one row per edge, one column with unique edge identifiers, and one column with the nodes contained in each edge. It may also contain additional columns holding further metadata associated with individual edges. Column names may differ between datasets to reflect dataset semantics.
3. Provide a unified loading interface to the datasets in Python.
4. Transform semantics-laden hypergraph CSV files into semantics-free one-based integer edge lists and sparse matrices for curvature computations in Julia, compute curvatures in Julia, and store the results in JSON files.
5. Map results back to original dataset semantics in Python for further examination.

In the following, we give more details on the provenance, semantics, and statistics of our datasets. Unless if otherwise noted, we make our datasets publicly available with our online materials, along with the raw data and all preprocessing code²

A.3.1 APS-A, APS-AV, APS-CV: AMERICAN PHYSICAL SOCIETY JOURNAL ARTICLES

The American Physical Society (APS), a nonprofit organization working to advance the knowledge of physics, publishes several peer-reviewed research journals. The APS makes two datasets based on its publications available to researchers: (i) an edge list containing (citing, cited) pairs of articles contained in its collection, and (ii) a JSON dataset containing the metadata for each article in its collection. These datasets are updated on a yearly basis, and researchers can request access by filling out a web form located at <https://journals.aps.org/datasets>. We made a data access request and were granted access to the 2021 versions of the APS datasets within two weeks.

From the APS datasets, we derived the following hypergraphs and hypergraph collections:

- (i) **aps-a**: Each node corresponds to an author who published at least one article in an APS journal. Each edge e corresponds to an article in an APS journal, and it contains as nodes all authors of e . This hypergraph is derived from the JSON data.
- (ii) **aps-av**: **aps-a**, split up by journal, for a total of 19 hypergraphs. For each journal j , the edge set of **aps-a** is restricted to articles from j , and the node set of **aps-a** is restricted to nodes authoring at least one article from j .
- (iii) **aps-cv**: We derive one hypergraph for each of the 19 journals represented in the edge list data. For each journal j , the edge set comprises articles from j citing at least one article in j , and the node set consists of articles in j cited by at least one article in j .

Access. Due to the terms and conditions associated with data access, we cannot make the APS datasets or the hypergraphs derived from them publicly available, and researchers seeking to work with this data will have to request data access from APS directly as outlined above. However, we make our preprocessing code publicly available, such that researchers who have obtained access to the APS datasets can easily reproduce our hypergraphs from the raw data.

Caveats. When doing our case studies on the **aps-cv** dataset, we observed that some DOIs present in the edge list had no associated metadata in the JSON files provided by APS. This does not affect our curvature computations, but it might constrain the interpretability of results, e.g., when inspecting node clustering results based on article categories present only in the metadata.

²<https://doi.org/10.5281/zenodo.7624573>

A.3.2 DBLP, DBLP-V: DBLP JOURNAL ARTICLES AND CONFERENCE PROCEEDINGS

The DBLP computer science library provides high-quality bibliographic information on computer science publications. All DBLP data is released under a CC0 license and freely available in one XML file that is updated regularly. We obtained the XML dump dated September 1, 2022 from <https://dblp.org/xml/release/> and preprocessed it into a CSV file containing only entries corresponding to the XML tags `article` and `inproceedings`, with one row per entry and the following columns:

- `key`: unique identifier of the entry, e.g., `conf/iclr/XuHLJ19` or `journals/cacm/Savage16c`.
- `tag`: XML tag associated with the entry, one of `{inproceedings, article}`.
- `crossref`: cross-reference to a venue, e.g., `conf/iclr/2019`. Sometimes missing although a venue should be present.
- `author`: semicolon-separated list of DBLP author names, e.g., `Keyulu Xu; Weihua Hu; Jure Leskovec; Stefanie Jegelka`. Sometimes missing (we discard entries without authors when loading the data).
- `year`: entry publication year, e.g., `2019`.
- `title`: entry title, e.g., `How Powerful are Graph Neural Networks?`.
- `publtype`: if present, the type of publication, e.g., `informal`. Mostly missing.
- `journal`: for article entries, the name of the publishing journal, e.g., `Commun. ACM`.
- `booktitle`: for inproceedings entries, the name of the publishing venue, e.g., `ICLR`.
- `volume`: if present, the publication volume, e.g., `59`.
- `number`: if present, the publication number, e.g., `7`.
- `pages`: if present, the entry pages, e.g., `12–14`.
- `mdate`: modification date, e.g., `2019-07-25`.

This constitutes our individual hypergraph `dblp`, in which each edge represents a paper, and each node represents an author. From this hypergraph, we additionally derived the `dblp-v` hypergraph collection, which contains different subsets of `dblp` by venue or group of venues. More precisely, we distinguish 1 193 hypergraphs as follows:

- (i) `dblp_journal-all, dblp_inproceedings-all`: partition of `dblp` into entries published in journals and entries published as part of proceedings.
- (ii) `dblp_journal-{journal}`: one hypergraph per journal, for all journals with at least 1 000 articles in the DBLP dataset.
- (iii) `dblp_proceedings-{venue}`: one hypergraph per venue (grouped by `booktitle`), for all venues with at least 1 000 papers in the DBLP dataset.
- (iv) `dblp_proceedings_area-{area}_{venues}`: one hypergraph per each of the FoR (field of research) areas 4601–4608, 4611–4613 as used in the CORE ranking (4609 and 4610 were not present in the ranking), where each area is represented by all conferences (grouped by `booktitle`) with CORE rank A* and A that have at least 1 000 papers in the DBLP dataset. These areas and associated top conferences are as follows:
 - 4601: Applied computing – AIED, ICCS
 - 4602: Artificial intelligence – AAI, AAMAS, ACL, AISTATS, CADE, CIKM, COLING, COLT, CP, CogSci, EACL, EC, ECAI, EMNLP, GECCO, ICAPS, IJCAI, IROS, KR, UAI
 - 4603: Computer vision and multimedia computation – AAI, CVPR, ECAI, ICCV, ICME, IJCAI, IROS, WACV
 - 4604: Cybersecurity and privacy – AsiaCCS, CCS, CRYPTO, DSN
 - 4605: Data management and data science – CIKM, ECIR, EDBT, ICDAR, ICDE, ICDM, ISWC, KDD, MSR, PODS, RecSys, SDM, SIGIR, VLDB, WSDM, WWW
 - 4606: Distributed computing and systems software – ASPLOS, CCGRID, CLUSTER, CONCUR, DISC, DSN, HPCA, HPDC, ICCAD, ICDCS, ICNP, ICPP, ICS, ICWS, IN-FOCOM, IPDPS, IPSN, PODC, SC, SIGCOMM, SPAA, WWW
 - 4607: Graphics, augmented reality and games – ISMAR, SIGGRAPH, VR, VRST

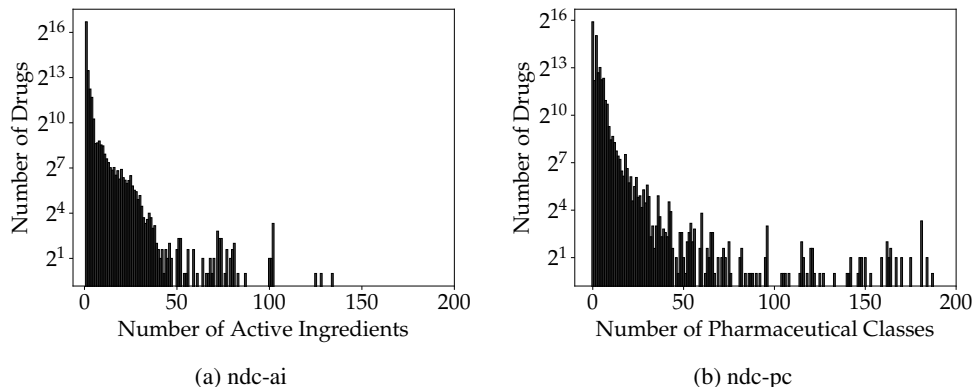


Figure 4: Edge cardinality distributions for hypergraphs derived from NDC data.

- 4608: Human-centred computing – ASSETS, CHI, CSCW, ITiCSE, IUI, SIGCSE, UIST
- 4611: Machine learning – AAAI, AISTATS, COLT, ECAI, ICDM, ICLR, ICML, IJCAI, KDD, NeurIPS, PPSN, WSDM
- 4612: Software engineering – ASE, ASPLOS, CAV, ICSE, ICST, ISCA, ISSRE, MSR, OOPSLA, PLDI, POPL, RE, SIGMETRICS
- 4613: Theory of computation – EC, ESA, FOCS, ICALP, ICLP, ISAAC, ISSAC, KR, LICS, MFCS, SODA, STACS, STOC, WG

Caveats. For about 0.1% of all records, our XML parser failed, which originally resulted in “None” as one of the authors of all problematic records. We then redid the preprocessing (and all subsequent computations) *excluding* those records, but the records were still counted when determining the venues to include in dblp-v.

A.3.3 NDC-AI, NDC-PC: DRUGS APPROVED BY THE U.S. FOOD & DRUG ADMINISTRATION

The U.S. Food and Drug Administration (FDA) collects information on all drugs manufactured, prepared, propagated, compounded, or processed by registered drug establishments for commercial distribution in the United States. The FDA maintains the National Drug Code (NDC) Directory, which is updated daily and contains the listed NDC numbers and all information submitted as part of a drug listing. We downloaded the NDC data from <https://download.open.fda.gov/drug/ndc/drug-ndc-0001-of-0001.json.zip> on August 21, 2022, and transformed it into a CSV file, an example record of which is shown in Table 3. From this CSV file, we derived two hypergraphs. In both hypergraphs, edges correspond to FDA-registered drugs. In *ndc-ai*, nodes correspond to the active ingredients used in these drugs, and in *ndc-pc*, nodes correspond to the pharmaceutical classes assigned to these drugs. The edge cardinality distributions resulting from both semantics are shown in Fig. 4.

A.3.4 MUS: MUSIC PIECES

music21 is an open-source Python library for computer-aided musicology that comes with a corpus of public-domain music in symbolic notation. Using the *music21* library, we extracted a collection of hypergraphs from the *music21* corpus. In this collection, each hypergraph corresponds to a music piece, each edge corresponds to a chord sounding for a specific duration at a particular offset from the start of the piece, and each node corresponds to a sound frequency. Note that hypergraphs in the *mus* collection are node-aligned, which distinguishes them from the hypergraphs in all other collections. In Table 4, we show the cardinality decomposition of selected music hypergraphs that include the largest edges. There, we include edges of cardinality 0 for completeness (they correspond to pauses in the music), but they are discarded in our curvature computations.

Caveats. When constructing our hypergraph collection from the *music21* corpus, we excluded pieces that are primarily monophonic. After exploring the corpus manually and evaluating the chord

Table 3: Example record from the data underlying the ndc-ai and ndc-pc hypergraphs.

Column Name	Record Value
product_ndc	71930-020
active_ingredients_names	[ACETAMINOPHEN, HYDROCODONE BITARTRATE]
active_ingredients_strengths	[325 mg/1, 7.5 mg/1]
pharm_class	[Opioid Agonist [EPC], Opioid Agonists [MoA]]
marketing_category	ANDA
dea_schedule	CII
finished	True
packaging	[{'package_ndc': '71930-020-12', 'description': '100 TABLET in 1 BOTTLE (71930-020-12)', 'marketing_start_date': '20180713', 'sample': False}, {'package_ndc': '71930-020-52', 'description': '500 TABLET in 1 BOTTLE (71930-020-52)', 'marketing_start_date': '20180713', 'sample': False}]
dosage_form	TABLET
product_type	HUMAN PRESCRIPTION DRUG
spl_id	58b53a57-388e-40d0-9985-048e5af09b0d
route	[ORAL]
product_id	71930-020_58b53a57-388e-40d0-9985-048e5af09b0d
application_number	ANDA210211
labeler_name	Eywa Pharma Inc
generic_name	Hydrocodone Bitartrate and Acetaminophen
brand_name	Hydrocodone Bitartrate and Acetaminophen
brand_name_base	Hydrocodone Bitartrate and Acetaminophen
brand_name_suffix	
listing_expiration_date	2022-12-31
marketing_start_date	2018-07-13
marketing_end_date	
openfda	{'manufacturer_name': ['Eywa Pharma Inc'], 'rxcur': ['856999', '857002', '857005'], 'spl_set_id': ['fcd2b59e-8087-475e-9e6b-911bd846ea96'], 'is_original_packager': [True], 'upc': ['0371930021121', '0371930020124', '0371930019128'], 'unii': ['NO70W886KK', '362O9ITL9D']}

statistics of individual pieces, we decided to use only music with the following prefixes (corresponding to names of composers or collections): bach, beethoven, chopin, haydn, handel, monteverdi, mozart, palestrina, schumann, schubert, verdi, joplin, trecento, weber. Some pieces are included in several editions (e.g., BWV 190.7, the chorale by Johann Sebastian Bach occupying the first two lines of Table 4, which is included in both the original and an instrumental version).

A.3.5 STEX: STACKEXCHANGE SITES

StackExchange is a platform hosting Q&A communities also known as sites. Each question is assigned at least one and at most five tags. In the second half of August 2022, we used the StackExchange API to download all questions asked on all StackExchange sites listed on the StackExchange data explorer (<https://data.stackexchange.com/>), along with their associated tags and other metadata (including question titles and, for smaller sites, also question bodies). From our downloads, we created the stex hypergraph collection, in which each hypergraph corresponds to a StackExchange site, each edge corresponds to a question asked on a site, and each node corresponds to a tag used at least once on a site. Tables 5 to 11 list the basic statistics for each hypergraph from the stex collection.

Caveats. While our curvature computations uniformly include only questions asked no later than August 15, midnight GMT, the metadata associated with these questions stems from snapshots at different times in the second half of August 2022. We also excluded `stackoverflow.com` and `math.stackexchange.com` from our downloads because they could not be downloaded within one day due to API quota limitations, and `ru.stackoverflow.com` because it was large but we would not have been able to interpret our results.

Table 4: Selection of hypergraphs from the mus collection. n is the number of nodes, m is the number of edges, and the columns labeled i for $i \in \{0, 1, \dots, 12\}$ record the number of edges of cardinality i in the hypergraph. Identifiers correspond to abbreviated `music21` identifiers and generally have the shape {composer}-{work identifier}-{suffix}, where o stands for *opus*, m stands for *movement*, and *inst* stands for *instrumental*.

	n	m	0	1	2	3	4	5	6	7	8	9	10	11	12
bach-bwv190.7-inst	38	233	1	0	0	4	25	60	56	72	9	6	0	0	0
bach-bwv190.7	38	233	1	0	0	4	25	60	56	72	9	6	0	0	0
bach-bwv248.23-2	35	155	1	0	0	12	45	90	0	3	1	2	1	0	0
bach-bwv248.42-4	38	386	3	1	11	42	147	106	54	14	7	1	0	0	0
beethoven-o133	88	5140	236	565	828	1515	1758	168	42	21	5	2	0	0	0
beethoven-o18no1-m1	70	1979	28	295	165	472	761	244	7	6	0	0	1	0	0
beethoven-o18no1-m4	77	2669	13	338	438	678	1032	134	33	1	1	1	0	0	0
beethoven-o18no4	81	4730	95	465	674	977	1940	521	50	3	3	1	1	0	0
beethoven-o59no1-m4	75	2338	27	80	231	338	1467	168	18	4	4	0	1	0	0
beethoven-o59no2-m1	86	2338	60	127	398	427	1065	203	18	30	4	5	0	0	1
beethoven-o59no3-m4	81	3292	19	381	529	734	1219	255	139	14	1	1	0	0	0
beethoven-o74	82	6492	112	440	922	1448	2886	538	119	21	5	1	0	0	0
monteverdi-madrigal.3.6	35	480	1	9	40	194	151	76	4	3	1	1	0	0	0
schumann-clara-o17-m3	63	819	5	12	133	208	151	108	83	74	25	13	5	2	0
schumann-o41no1-m5	72	2410	51	130	208	592	919	366	117	18	2	4	0	2	1

A.3.6 SHA: SHAKESPEARE’S PLAYS

The sha collection is a subset of the HYPERBARD dataset recently introduced by Coupette et al. (2022), based on the TEI-encoded XML files of Shakespeare’s plays provided by Folger Digital Texts. Here, each hypergraph represents one of Shakespeare’s plays, which are categorized into three types: comedy, history, and tragedy. In each hypergraph representing a play, nodes correspond to named characters in the play, and edges correspond to groups of characters simultaneously present on stage. These hypergraphs are documented extensively in the paper introducing the HYPERBARD dataset (Coupette et al., 2022).

A.3.7 SYN-C, SYN-R, SYN-S: SYNTHETIC HYPERGRAPHS

To generate synthetic hypergraphs, we wrote hypergraph generators extending three well-known graph models to hypergraphs.

- (i) For `syn-c`, we extended the configuration model, which, for undirected graphs, is specified by a degree sequence. Our hypergraph configuration model is specified by a node degree sequence and an edge cardinality sequence.
- (ii) For `syn-r`, we extended the Erdős-Rényi random graph model, which, for undirected graphs, is specified by a number of nodes n and an edge existence probability p . Our Erdős-Rényi random hypergraph model is specified by a number of nodes n , a number of edges m , and the probability p of a one in any cell of the node-to-edge incidence matrix.
- (iii) For `syn-s`, we extended the stochastic block model which, for undirected graphs, is specified by a vector of c community sizes and a $c \times c$ affinity matrix specifying affiliation probabilities between communities. Our hypergraph stochastic block model is specified by a vector of c_V node community sizes, a vector of c_E edge community sizes, and a $c_V \times c_E$ affinity matrix specifying affiliation probabilities between node communities and edge communities.

We used each of our generators to create 250 hypergraphs with identical node count n , edge count m , and density c/nm , where c is the number of filled cells in the node-to-edge incidence matrix.

Caveats. Our generators work by pairing node and edge indices, and duplicated (node, edge) index pairs are discarded to generate simple hypergraphs, which can lead to small deviations from the input specification in practice.

Table 5: Basic statistics of hypergraphs derived from StackExchange sites. n is the number of nodes, m is the number of edges, and columns labeled $i \in [5]$ count edges of cardinality i .

	n	m	n/m	1	2	3	4	5
3dprinting	416	4 902	0.084863	1 003	1 617	1 367	649	266
3dprinting.meta	45	197	0.228426	65	85	38	5	4
academia	457	39 270	0.011637	6 428	11 831	11 360	6 294	3 357
academia.meta	91	1 237	0.073565	396	486	249	95	11
ai	980	10 204	0.096041	767	1 805	2 696	2 427	2 509
ai.meta	49	315	0.155556	100	132	67	11	5
alcohol	154	1 138	0.135325	415	406	229	56	32
alcohol.meta	28	94	0.297872	28	42	14	8	2
android	1 517	56 403	0.026896	12 890	18 313	14 406	6 996	3 798
android.meta	103	996	0.103414	159	447	281	97	12
anime	1 528	12 122	0.126052	9 510	2 215	348	43	6
anime.meta	83	900	0.092222	234	384	215	56	11
apple	969	121 999	0.007943	15 822	34 777	37 243	22 652	11 505
apple.meta	108	1 452	0.074380	354	601	393	90	14
arduino	445	23 616	0.018843	5 838	7 357	6 027	2 858	1 536
arduino.meta	50	255	0.196078	101	110	34	10	0
askubuntu	3 137	393 266	0.007977	68 310	104 529	105 601	68 907	45 919
astronomy	566	12 773	0.044312	2 781	3 812	3 284	1 777	1 119
astronomy.meta	63	339	0.185841	115	93	76	43	12
aviation	1 024	22 701	0.045108	4 294	7 193	6 384	3 231	1 599
aviation.meta	73	752	0.097074	247	295	155	46	9
bicycles	548	18 873	0.029036	4 884	6 267	4 652	2 097	973
bicycles.meta	74	442	0.167421	150	197	76	15	4
bioacoustics	354	287	1.233449	20	50	101	54	62
bioacoustics.meta	36	49	0.734694	4	24	16	5	0
bioinformatics	490	4 998	0.098039	922	1 420	1 335	782	539
bioinformatics.meta	29	112	0.258929	44	53	15	0	0
biology	745	27 348	0.027241	5 487	8 618	7 093	3 742	2 408
biology.meta	88	814	0.108108	280	331	145	44	14
bitcoin	936	28 882	0.032408	6 677	8 927	7 432	3 766	2 080
bitcoin.meta	58	434	0.133641	142	202	71	16	3
blender	371	98 724	0.003758	31 012	30 861	22 200	9 614	5 037
blender.meta	69	716	0.096369	273	291	108	35	9
boardgames	1 000	13 166	0.075953	9 800	2 779	500	75	12
boardgames.meta	75	659	0.113809	197	289	144	27	2
bricks	202	4 220	0.047867	1 391	1 669	805	266	89
bricks.meta	52	211	0.246445	45	95	51	17	3
buddhism	487	7 956	0.061212	2 381	2 357	1 730	896	592
buddhism.meta	59	491	0.120163	104	252	94	30	11
cardano	285	2 248	0.126779	585	664	548	277	174
cardano.meta	24	43	0.558140	18	15	10	0	0
chemistry	370	41 571	0.008900	9 725	14 183	10 803	4 790	2 070
chemistry.meta	90	1 034	0.087041	250	441	243	88	12
chess	387	7 864	0.049212	1 646	2 682	2 069	985	482
chess.meta	62	368	0.168478	102	183	72	9	2
chinese	166	10 298	0.016120	4 467	3 438	1 628	543	222
chinese.meta	60	349	0.171920	93	170	67	12	7
christianity	1 129	14 955	0.075493	1 739	3 571	4 205	2 967	2 473
christianity.meta	110	1 579	0.069664	593	589	285	88	24
civicism	507	14 324	0.035395	4 639	5 150	3 085	1 083	367
civicism.meta	18	69	0.260870	43	18	6	2	0
codegolf	257	13 228	0.019428	1 360	4 586	4 379	2 106	797
codegolf.meta	128	2 276	0.056239	559	848	549	245	75
codereview	1 114	76 105	0.014638	6 306	20 542	23 777	16 106	9 374
codereview.meta	133	1 947	0.068310	190	615	688	345	109

Table 6: Basic statistics of hypergraphs derived from StackExchange sites (continued). n is the number of nodes, m is the number of edges, and columns labeled $i \in [5]$ count edges of cardinality i .

	n	m	n/m	1	2	3	4	5
coffee	114	1 381	0.082549	492	524	260	78	27
coffee.meta	27	90	0.300000	45	30	13	2	0
communitybuilding	74	559	0.132379	148	219	112	55	25
communitybuilding.meta	27	132	0.204545	36	67	24	4	1
computergraphics	259	3 600	0.071944	883	1 024	877	489	327
computergraphics.meta	34	150	0.226667	55	66	27	2	0
conlang	96	448	0.214286	109	204	91	32	12
conlang.meta	21	61	0.344262	16	34	7	4	0
cooking	834	25 877	0.032229	6 568	9 266	6 344	2 682	1 017
cooking.meta	83	866	0.095843	241	410	178	34	3
craftcms	523	13 756	0.038020	3 738	4 912	3 410	1 263	433
craftcms.meta	20	50	0.400000	22	11	15	1	1
crafts	193	2 039	0.094654	706	828	397	84	24
crafts.meta	49	184	0.266304	40	88	45	11	0
crypto	506	27 447	0.018436	6 448	9 056	6 960	3 283	1 700
crypto.meta	74	542	0.136531	139	237	127	27	12
cs	656	44 794	0.014645	8 624	14 332	12 644	6 336	2 858
cs.meta	86	603	0.142620	90	247	185	68	13
cseducators	210	1 080	0.194444	297	378	252	116	37
cseducators.meta	29	146	0.198630	52	68	26	0	0
cstheory	498	11 959	0.041642	1 653	3 384	3 495	2 052	1 375
cstheory.meta	80	608	0.131579	157	262	156	30	3
datascience	663	33 997	0.019502	4 110	8 028	9 305	6 753	5 801
datascience.meta	51	237	0.215190	80	97	38	16	6
dba	1 197	96 887	0.012355	15 956	29 750	27 361	15 610	7 682
dba.meta	76	800	0.095000	280	334	140	38	8
devops	431	5 025	0.085771	1 070	1 647	1 340	616	352
devops.meta	40	144	0.277778	45	63	31	5	0
diy	919	71 007	0.012942	19 347	22 079	17 371	8 399	3 811
diy.meta	68	603	0.112769	227	233	118	21	4
drones	220	731	0.300958	114	240	193	115	69
drones.meta	28	62	0.451613	11	31	17	3	0
drupal	149	86 283	0.001727	25 218	37 599	18 867	4 075	524
drupal.meta	75	1 014	0.073964	361	432	186	35	0
dsp	509	24 850	0.020483	4 460	6 779	6 565	4 081	2 965
dsp.meta	48	307	0.156352	153	108	30	14	2
earthscience	424	6 329	0.066993	1 111	1 778	1 698	1 094	648
earthscience.meta	54	321	0.168224	100	145	63	12	1
ebooks	180	1 466	0.122783	364	489	339	163	111
ebooks.meta	39	99	0.393939	31	37	23	6	2
economics	494	13 690	0.036085	3 488	4 426	3 160	1 678	938
economics.meta	60	444	0.135135	241	151	40	7	5
electronics	2 318	175 731	0.013191	31 201	46 423	46 974	29 107	22 026
electronics.meta	107	1 685	0.063501	698	628	282	62	15
elementaryos	314	8 471	0.037068	3 043	2 910	1 669	619	230
elementaryos.meta	29	107	0.271028	60	28	17	2	0
ell	533	99 970	0.005332	46 764	31 310	14 644	5 147	2 105
ell.meta	93	1 224	0.075980	448	489	226	52	9
emacs	891	23 939	0.037220	7 561	9 371	4 980	1 590	437
emacs.meta	51	216	0.236111	34	112	59	10	1
engineering	468	13 867	0.033749	3 582	4 121	3 315	1 770	1 079
engineering.meta	47	217	0.216590	71	87	45	10	4
english	984	125 848	0.007819	48 232	38 850	23 112	10 111	5 543
english.meta	182	3 589	0.050711	1 224	1 305	733	249	78
eosio	241	2 422	0.099505	766	766	533	245	112

Table 7: Basic statistics of hypergraphs derived from StackExchange sites (continued). n is the number of nodes, m is the number of edges, and columns labeled $i \in [5]$ count edges of cardinality i .

	n	m	n/m	1	2	3	4	5
eosio.meta	19	27	0.703704	6	14	4	2	1
es.meta.stackoverflow	168	1 817	0.092460	310	665	568	230	44
es.stackoverflow	2 960	179 452	0.016495	38 027	58 218	47 343	23 415	12 449
esperanto	99	1 592	0.062186	1 050	422	96	16	8
esperanto.meta	20	84	0.238095	37	38	9	0	0
ethereum	891	46 678	0.019088	8 449	12 402	12 327	7 687	5 813
ethereum.meta	63	259	0.243243	98	71	59	26	5
expatriates	304	7 182	0.042328	1 068	2 178	2 163	1 156	617
expatriates.meta	48	157	0.305732	41	72	41	2	1
expressionengine	603	12 447	0.048445	3 724	4 239	2 901	1 150	433
expressionengine.meta	35	123	0.284553	59	49	15	0	0
fitness	402	9 667	0.041585	2 123	2 864	2 427	1 289	964
fitness.meta	54	315	0.171429	126	123	57	7	2
freelancing	125	1 946	0.064234	632	654	394	177	89
freelancing.meta	33	132	0.250000	36	64	25	5	2
french	324	12 413	0.026102	3 368	4 126	2 923	1 390	606
french.meta	73	290	0.251724	58	127	80	24	1
gamedev	1 096	54 182	0.020228	7 381	16 130	15 996	9 433	5 242
gamedev.meta	78	910	0.085714	300	430	148	27	5
gaming	5 883	98 355	0.059814	72 655	20 708	4 120	758	114
gaming.meta	177	4 062	0.043575	478	1 853	1 219	425	87
gardening	526	16 629	0.031631	3 725	5 390	4 122	2 097	1 295
gardening.meta	60	320	0.187500	95	157	49	17	2
genealogy	465	3 572	0.130179	421	742	1 037	902	470
genealogy.meta	56	485	0.115464	133	273	70	8	1
german	265	16 022	0.016540	6 003	5 915	2 914	927	263
german.meta	69	540	0.127778	177	224	107	30	2
gis	2 829	150 205	0.018834	13 868	36 527	45 339	32 527	21 944
gis.meta	91	1 016	0.089567	174	361	317	125	39
graphicdesign	612	34 820	0.017576	7 542	10 789	9 364	4 821	2 304
graphicdesign.meta	83	851	0.097532	253	338	187	58	15
ham	334	4 299	0.077692	927	1 287	1 199	610	276
ham.meta	45	156	0.288462	39	65	32	18	2
hardwarerecs	246	3 945	0.062357	1 201	1 366	823	378	177
hardwarerecs.meta	42	255	0.164706	81	100	58	16	0
hermeneutics	422	12 563	0.033591	2 819	3 720	3 074	1 772	1 178
hermeneutics.meta	63	581	0.108434	256	212	84	22	7
hinduism	825	15 771	0.052311	2 597	4 337	3 976	2 876	1 985
hinduism.meta	89	827	0.107618	196	295	200	98	38
history	843	13 784	0.061158	2 071	3 757	3 839	2 436	1 681
history.meta	68	746	0.091153	340	265	107	31	3
homebrew	415	6 113	0.067888	1 393	1 976	1 593	803	348
homebrew.meta	50	172	0.290698	67	63	35	4	3
hsm	252	3 898	0.064649	982	1 272	928	464	252
hsm.meta	32	146	0.219178	61	44	37	4	0
interpersonal	280	3 890	0.071979	342	1 030	1 307	790	421
interpersonal.meta	76	825	0.092121	214	328	205	62	16
iot	241	2 103	0.114598	560	754	504	193	92
iot.meta	36	136	0.264706	30	74	27	5	0
iota	148	1 023	0.144673	300	352	248	84	39
iota.meta	18	38	0.473684	10	20	8	0	0
islam	562	13 792	0.040748	3 018	4 990	3 557	1 519	708
islam.meta	103	864	0.119213	240	358	206	47	13
italian	94	3 590	0.026184	1 296	1 376	636	206	76
italian.meta	27	151	0.178808	77	57	14	2	1

Table 8: Basic statistics of hypergraphs derived from StackExchange sites (continued). n is the number of nodes, m is the number of edges, and columns labeled $i \in [5]$ count edges of cardinality i .

	n	m	n/m	1	2	3	4	5
ja.meta.stackoverflow	74	1 115	0.066368	193	386	306	204	26
ja.stackoverflow	1 145	28 785	0.039778	10 077	10 518	5 624	1 946	620
japanese	354	26 365	0.013427	9 325	8 869	5 191	2 020	960
japanese.meta	75	817	0.091799	270	351	147	43	6
joomla	374	7 190	0.052017	1 289	2 221	2 058	1 072	550
joomla.meta	41	150	0.273333	81	46	19	4	0
judaism	1 264	36 511	0.034620	3 753	8 116	10 854	8 042	5 746
judaism.meta	147	1 455	0.101031	108	576	489	222	60
korean	118	1 716	0.068765	767	596	264	69	20
korean.meta	30	80	0.375000	38	28	8	5	1
languagelearning	216	1 287	0.167832	225	466	354	176	66
languagelearning.meta	52	195	0.266667	31	103	48	12	1
latin	370	5 400	0.068519	1 223	1 603	1 371	797	406
latin.meta	46	192	0.239583	34	80	49	25	4
law	938	23 649	0.039663	4 483	7 573	6 329	3 381	1 883
law.meta	66	499	0.132265	117	216	120	36	10
lifehacks	140	2 928	0.047814	1 024	1 052	595	190	67
lifehacks.meta	59	268	0.220149	65	122	72	6	3
linguistics	605	10 003	0.060482	1 947	2 836	2 556	1 627	1 037
linguistics.meta	59	363	0.162534	118	159	58	23	5
literature	2 335	5 614	0.415924	703	1 621	2 249	830	211
literature.meta	63	462	0.136364	56	292	99	15	0
magento	1 811	110 316	0.016416	15 598	28 805	32 671	20 873	12 369
magento.meta	66	575	0.114783	251	227	78	17	2
martialarts	205	2 199	0.093224	461	696	529	326	187
martialarts.meta	40	218	0.183486	66	97	46	9	0
math.meta	232	9 169	0.025303	1 051	3 485	2 919	1 312	402
matheducators	225	3 360	0.066964	696	1 118	903	435	208
matheducators.meta	57	255	0.223529	64	119	61	8	3
mathematica	705	85 069	0.008287	25 896	31 653	18 182	6 542	2 796
mathematica.meta	75	914	0.082057	416	341	130	25	2
mathoverflow.net	1 530	137 735	0.011108	20 381	37 763	38 643	24 597	16 351
mattermodeling	449	2 422	0.185384	169	547	668	495	543
mattermodeling.meta	61	142	0.429577	25	41	29	37	10
mechanics	1 430	25 243	0.056649	4 196	6 245	7 592	4 673	2 537
mechanics.meta	52	387	0.134367	124	182	66	13	2
medicalsciences	1 435	7 586	0.189164	1 423	1 970	1 754	1 261	1 178
medicalsciences.meta	65	501	0.129741	171	191	102	27	10
meta.askubuntu	196	5 698	0.034398	1 625	2 308	1 257	397	111
meta	1 250	97 114	0.012871	4 599	25 289	34 007	23 233	9 986
meta.mathoverflow.net	133	1 687	0.078838	272	601	504	229	81
meta.serverfault	139	2 173	0.063967	767	799	463	119	25
meta.stackoverflow	622	47 387	0.013126	5 297	15 301	15 792	8 233	2 764
meta.superuser	207	5 000	0.041400	1 010	1 914	1 474	510	92
monero	400	4 285	0.093349	1 193	1 424	969	481	218
monero.meta	23	85	0.270588	40	26	19	0	0
money	1 002	36 187	0.027690	3 788	8 036	10 340	8 450	5 573
money.meta	67	672	0.099702	220	260	147	40	5
movies	4 537	21 829	0.207843	4 857	11 430	4 546	877	119
movies.meta	75	1 285	0.058366	302	519	391	63	10
music	516	23 424	0.022029	4 754	7 644	6 370	3 117	1 539
music.meta	81	992	0.081653	391	387	166	40	8
musicfans	237	2 990	0.079264	1 209	1 169	465	111	36
musicfans.meta	42	218	0.192661	62	95	38	18	5
mythology	303	1 953	0.155146	484	723	439	215	92

Table 9: Basic statistics of hypergraphs derived from StackExchange sites (continued). n is the number of nodes, m is the number of edges, and columns labeled $i \in [5]$ count edges of cardinality i .

	n	m	n/m	1	2	3	4	5
mythology.meta	35	162	0.216049	43	87	31	1	0
networkengineering	453	15 624	0.028994	2 988	4 240	3 835	2 496	2 065
networkengineering.meta	53	375	0.141333	192	115	48	17	3
opendata	302	5 990	0.050417	1 562	2 002	1 492	670	264
opendata.meta	26	180	0.144444	73	76	30	1	0
opensource	203	4 226	0.048036	845	1 442	1 094	528	317
opensource.meta	53	225	0.235556	35	109	61	19	1
or	255	2 865	0.089005	351	809	848	496	361
or.meta	44	114	0.385965	21	61	23	5	4
outdoors	555	5 908	0.093940	934	2 017	1 791	806	360
outdoors.meta	52	512	0.101562	169	276	60	7	0
parenting	304	6 636	0.045811	1 182	2 175	1 873	1 004	402
parenting.meta	61	473	0.128964	96	217	125	31	4
patents	2 102	4 381	0.479799	1 421	1 211	879	481	389
patents.meta	46	167	0.275449	55	69	34	8	1
pets	289	7 874	0.036703	781	2 706	2 350	1 305	732
pets.meta	62	407	0.152334	60	194	112	26	15
philosophy	606	17 915	0.033826	4 898	5 399	4 079	2 089	1 450
philosophy.meta	61	793	0.076923	355	258	127	38	15
photo	1 156	25 961	0.044528	3 395	6 960	7 848	4 936	2 822
photo.meta	107	1 095	0.097717	289	500	239	60	7
physics	892	209 515	0.004257	21 914	42 808	53 150	45 705	45 938
physics.meta	114	3 228	0.035316	713	1 085	872	403	155
pm	283	6 198	0.045660	1 379	1 850	1 592	870	507
pm.meta	64	315	0.203175	81	129	73	27	5
poker	131	2 051	0.063871	763	659	372	181	76
poker.meta	29	122	0.237705	74	30	15	3	0
politics	793	14 628	0.054211	1 294	4 022	4 663	3 062	1 587
politics.meta	80	1 067	0.074977	249	436	259	103	20
portuguese	169	2 349	0.071946	703	898	509	174	65
portuguese.meta	35	137	0.255474	45	61	25	5	1
proofassistants	223	434	0.513825	80	175	116	42	21
proofassistants.meta	37	64	0.578125	11	26	18	7	2
psychology	401	7 641	0.052480	1 632	2 229	1 971	1 115	694
psychology.meta	62	557	0.111311	199	237	90	25	6
pt.meta.stackoverflow	140	2 986	0.046885	703	1 081	775	362	65
pt.stackoverflow	2 936	152 483	0.019255	28 143	50 055	42 386	21 287	10 612
puzzling	209	24 985	0.008365	6 912	9 471	5 731	2 020	851
puzzling.meta	98	1 365	0.071795	351	582	309	97	26
quant	693	20 283	0.034167	3 329	5 345	5 392	3 556	2 661
quant.meta	47	252	0.186508	95	115	37	3	2
quantumcomputing	306	7 823	0.039115	1 124	2 585	2 475	1 105	534
quantumcomputing.meta	50	187	0.267380	50	73	43	18	3
raspberrypi	598	35 872	0.016670	7 901	11 252	9 351	4 765	2 603
raspberrypi.meta	61	451	0.135255	213	169	58	8	3
retrocomputing	546	4 976	0.109727	925	1 694	1 366	692	299
retrocomputing.meta	70	304	0.230263	30	188	56	27	3
reverseengineering	347	8 754	0.039639	1 878	2 693	2 172	1 249	762
reverseengineering.meta	37	150	0.246667	56	62	28	3	1
robotics	276	6 261	0.044082	1 528	1 850	1 519	806	558
robotics.meta	39	159	0.245283	52	71	28	8	0
rpg	1 247	46 635	0.026740	4 236	12 463	15 431	9 542	4 963
rpg.meta	150	2 627	0.057099	310	986	844	379	108
ru.meta.stackoverflow	242	4 613	0.052460	445	1 312	1 574	979	303
rus	390	20 999	0.018572	12 276	5 131	2 341	840	411

Table 10: Basic statistics of hypergraphs derived from StackExchange sites (continued). n is the number of nodes, m is the number of edges, and columns labeled $i \in [5]$ count edges of cardinality i .

	n	m	n/m	1	2	3	4	5
rus.meta	30	214	0.140187	92	81	37	4	0
russian	166	4 516	0.036758	2 407	1 337	552	180	40
russian.meta	37	176	0.210227	80	61	25	7	3
salesforce	2 085	124 492	0.016748	22 537	37 977	33 635	19 220	11 123
salesforce.meta	79	795	0.099371	412	246	118	18	1
scicomp	346	10 381	0.033330	1 905	3 156	2 883	1 566	871
scicomp.meta	48	215	0.223256	75	90	42	8	0
scifi	3 693	69 344	0.053256	17 338	26 498	17 146	6 584	1 778
scifi.meta	149	3 265	0.045636	506	1 560	889	266	44
security	1 253	65 817	0.019038	11 950	19 799	18 266	9 809	5 993
security.meta	101	1 124	0.089858	311	507	242	52	12
serverfault	3 864	314 342	0.012292	40 967	83 417	92 763	60 560	36 635
sharepoint	1 722	99 911	0.017235	16 092	27 312	28 073	17 305	11 129
sharepoint.meta	78	581	0.134251	206	233	127	14	1
sitecore	362	11 395	0.031768	5 106	4 265	1 611	342	71
sitecore.meta	24	202	0.118812	40	60	99	3	0
skeptics	682	10 700	0.063738	2 227	4 165	2 952	1 042	314
skeptics.meta	100	1 529	0.065402	528	605	310	77	9
softwareengineering	1 674	61 392	0.027267	8 950	17 773	17 580	10 572	6 517
softwareengineering.meta	165	2 611	0.063194	421	1 023	776	310	81
softwarerecs	962	21 792	0.044145	3 090	6 533	6 199	3 723	2 247
softwarerecs.meta	85	654	0.129969	86	297	189	66	16
sound	1 224	9 786	0.125077	2 122	2 717	2 330	1 624	993
sound.meta	42	160	0.262500	65	66	25	1	3
space	1 203	17 392	0.069170	1 672	4 012	4 924	3 712	3 072
space.meta	74	682	0.108504	205	237	150	63	27
spanish	274	8 592	0.031890	2 276	2 722	2 140	1 010	444
spanish.meta	84	498	0.168675	94	216	135	42	11
sports	261	5 730	0.045550	926	2 371	1 637	609	187
sports.meta	57	350	0.162857	76	170	82	21	1
sqa	462	11 242	0.041096	2 263	3 250	2 881	1 705	1 143
sqa.meta	41	211	0.194313	115	71	17	7	1
stackapps	210	2 756	0.076197	277	858	883	514	224
stats	1 572	196 835	0.007986	19 622	47 967	57 502	41 443	30 301
stats.meta	132	1 685	0.078338	327	576	491	198	93
stellar	115	1 493	0.077026	585	438	298	109	63
stellar.meta	19	31	0.612903	9	14	8	0	0
substrate	512	1 814	0.282249	366	563	491	260	134
substrate.meta	40	44	0.909091	6	21	13	2	2
superuser	5 676	480 854	0.011804	64 273	127 561	135 549	91 137	62 334
sustainability	234	2 012	0.116302	431	713	536	235	97
sustainability.meta	37	151	0.245033	38	75	32	6	0
tex	2 035	237 763	0.008559	60 247	84 998	59 476	23 747	9 295
tex.meta	163	2 277	0.071585	389	921	671	235	61
tezos	210	1 828	0.114880	567	605	380	180	96
tezos.meta	18	32	0.562500	7	15	8	1	1
tor	218	5 636	0.038680	1 888	1 817	1 147	464	320
tor.meta	43	163	0.263804	57	76	25	4	1
travel	1 916	45 040	0.042540	2 985	8 914	13 809	11 528	7 804
travel.meta	99	1 379	0.071791	293	567	406	98	15
tridion	274	7 234	0.037877	1 471	2 758	1 915	818	272
tridion.meta	14	138	0.101449	93	39	6	0	0
ukrainian	124	2 094	0.059217	664	873	404	127	26
ukrainian.meta	33	104	0.317308	21	45	31	6	1
unix	2 777	220 644	0.012586	29 059	61 964	66 657	40 340	22 624

Table 11: Basic statistics of hypergraphs derived from StackExchange sites (continued). n is the number of nodes, m is the number of edges, and columns labeled $i \in [5]$ count edges of cardinality i .

	n	m	n/m	1	2	3	4	5
unix.meta	118	1 668	0.070743	367	727	407	144	23
ux	1 032	31 459	0.032805	4 660	8 934	8 823	5 530	3 512
ux.meta	94	899	0.104561	273	358	199	54	15
vegetarianism	115	677	0.169867	85	233	205	106	48
vegetarianism.meta	41	133	0.308271	26	62	32	13	0
vi	421	12 558	0.033524	4 494	4 802	2 358	694	210
vi.meta	35	201	0.174129	63	105	30	3	0
video	327	8 661	0.037755	2 705	2 693	1 831	882	550
video.meta	41	200	0.205000	63	96	32	8	1
webapps	951	33 202	0.028643	14 343	11 667	5 160	1 435	597
webapps.meta	106	937	0.113127	97	447	311	76	6
webmasters	1 078	36 840	0.029262	5 772	10 197	10 531	6 286	4 054
webmasters.meta	70	649	0.107858	202	258	135	45	9
windowsphone	287	3 440	0.083430	975	1 257	801	306	101
windowsphone.meta	44	148	0.297297	47	64	27	8	2
woodworking	244	3 739	0.065258	1 129	1 270	880	347	113
woodworking.meta	34	142	0.239437	69	46	25	2	0
wordpress	702	112 778	0.006225	27 669	37 039	28 491	13 228	6 351
wordpress.meta	82	866	0.094688	381	330	118	30	7
workplace	498	30 369	0.016398	6 371	9 325	8 103	4 221	2 349
workplace.meta	113	1 829	0.061782	506	699	447	150	27
worldbuilding	675	34 358	0.019646	2 958	8 284	10 839	7 267	5 010
worldbuilding.meta	120	2 032	0.059055	445	901	511	147	28
writing	391	11 699	0.033422	2 456	3 869	3 055	1 557	762
writing.meta	88	789	0.111534	145	415	173	49	7

A.4 IMPLEMENTATION DETAILS

To simplify the computation of Wasserstein distances between adjacent nodes, we leverage the following fact about the relevant distances (i.e., transportation costs) between nodes.

Lemma 1. *Given a hypergraph $H = (V, E)$ and nodes $i, j, k, \ell \in V$ with $i \sim j$ as well as $\mu_i(k) > 0$ and $\mu_j(\ell) > 0$, $d(k, \ell) \leq 3$.*

Proof. By the triangle inequality and the definition of our probability measures, we have

$$d(k, \ell) \leq d(k, i) + d(i, j) + d(j, \ell) = 3 .$$

□

Furthermore, we speed up the computation of Wasserstein distances by exploiting the following observation to reduce each instance to its smallest equivalent instance.

Lemma 2. *Given a hypergraph $H = (V, E)$ and nodes $i, j \in V$ with $i \sim j$, if $\mu_i(k) = \mu_j(k)$ for some node $k \in V$, then $W_1(\mu_i, \mu_j) = W_1(\mu_i^{-k}, \mu_j^{-k})$, where μ_i^{-k} is defined as*

$$\mu_i^{-k}(j) := \begin{cases} 0 & j = k \\ \mu_i(j) & j \neq k . \end{cases}$$

Proof. If $\mu_i(k) = \mu_j(k) = 0$, the claim holds trivially. Otherwise, $\mu_i(k) = \mu_j(k) = \beta > 0$. In this case, let C^* be an optimal coupling between μ_i and μ_j . If the probability mass allocated to k by μ_i does not get moved at all in C^* , it contributes 0 to $W_1(\mu_i, \mu_j)$, and we are done. Therefore, assume otherwise. Then there exist nodes $p, q \in V$ such that probability mass gets moved from p to k and from k to q in C^* . By the triangle inequality, $d(p, q) \leq d(p, k) + d(k, q)$, and as $d(k, k) = 0$, the cost of moving that mass directly from p to q and keeping all mass at k cannot be larger than the cost of moving the mass from p to k and from k to q . Hence, we can modify C^* such that the mass allocated to k by μ_i does not get moved at all without increasing the coupling cost. Thus, there always exists an optimal coupling in which all mass at k remains at k , and the claim follows. □

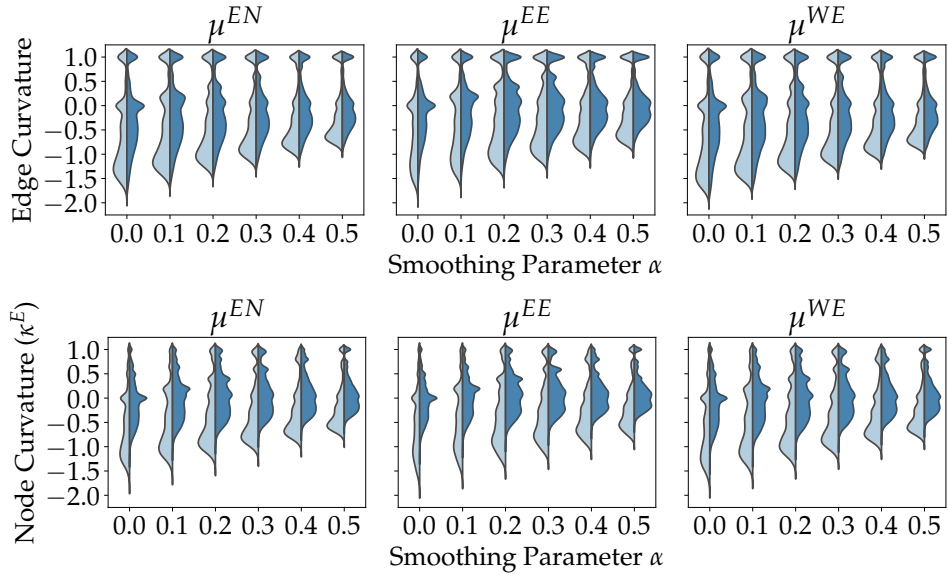
A.5 FURTHER RESULTS

Here, we showcase further results to support and supplement the exposition in the main paper.

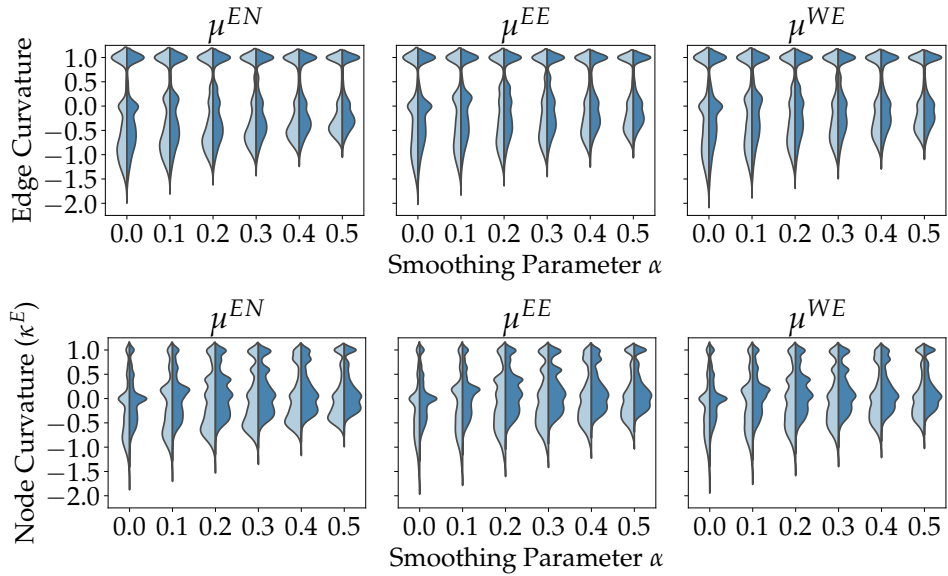
Q1 Parametrization. Expanding the discussion on ORCHID parametrizations, Fig. 5 shows the distributions of edge curvatures and edge-averaged node curvatures for two hypergraphs from the dblp-v collection, representing top conferences in machine learning and theoretical computer science, respectively. The figure highlights once more the consistently concentrating effect of increasing α , and it elucidates the differential effects of moving from maximum aggregation (left parts of the split violins) to mean aggregation (right parts of the split violins), from almost no shifts to large shifts in probability mass (compare, e.g., Fig. 5b, top right panel, with Fig. 5b, bottom left panel). Fig. 5 might convey the impression that, other parameters being equal, the distributions of curvatures based on μ^{EN} and μ^{WE} are more similar to each other than to μ^{EE} . This does not hold in general, however, as demonstrated for ndc-pc in Fig. 6a, where node curvature distributions based on μ^{WE} are more similar to those based on μ^{EE} than to the node curvature distributions based on μ^{EN} . Comparing Fig. 6a to Fig. 6b (ndc-ai), we further observe that rather similar distributions of edge curvature and directional curvature can be accompanied by rather different distributions of edge-averaged and direction-averaged node curvatures, even for hypergraphs originating from the same domain. Finally, when visualizing curvatures for hypergraphs in the same collection or across collections with related semantics (Fig. 7), we can identify several distinct prototypical shapes of curvature distributions and relationships between curvatures based on different probability measures.

Q2 Hypergraph Exploration. Extending the discussion of individual hypergraph exploration in the main paper, we focus on a case study of the citation hypergraph of the journal Physical Review E (PRE), which regularly publishes, inter alia, interdisciplinary work on graphs and networks. In this hypergraph, which has 45 504 nodes and 52 574 edges, nodes represent PRE articles *cited* by at least one other PRE article, edges represent PRE articles *citing* at least one other PRE article, and each edge i comprises the nodes j cited by the paper corresponding to i . Therefore, the *edge* curvature of a (citing) paper i can be interpreted as an indicator of its *breadth of content*: The more *positive* the edge curvature, the stronger the general tendency of the papers jointly cited by paper i to be cited together, suggesting that these papers are topically related. Similarly, the *node* curvature of a (cited) paper j can be interpreted as an indicator of its *breadth of impact*: The more *negative* the node curvature, the more diversely the paper has been cited in the literature.

With these interpretations in mind, we compute all curvatures for the PRE citation hypergraph, using $\alpha = 0.1$, μ^{WE} , and AGGA . We find that for all 54 articles with at least 100 citations (top articles), the edge-averaged node curvature is larger than the direction-averaged node curvature, which is always negative, although only 36% of all PRE articles exhibit this feature combination. This matches the intuition that from highly cited articles, the literature should diverge in many different directions. At the same time, we observe that curvatures span a considerable range, even among top articles. In Table 12, we record the top articles with extreme curvature values, and in Fig. 8, we display the pairwise relationships between curvature features and other local features for *all* PRE articles. In line with the interpretations sketched above, the top article with the largest node curvatures is a classic reference for community detection in the highly integrated field of network science, whereas the articles with the smallest node curvatures address topics relevant to a broader range of approaches to collective phenomena in many-body systems (which are the focus of PRE).

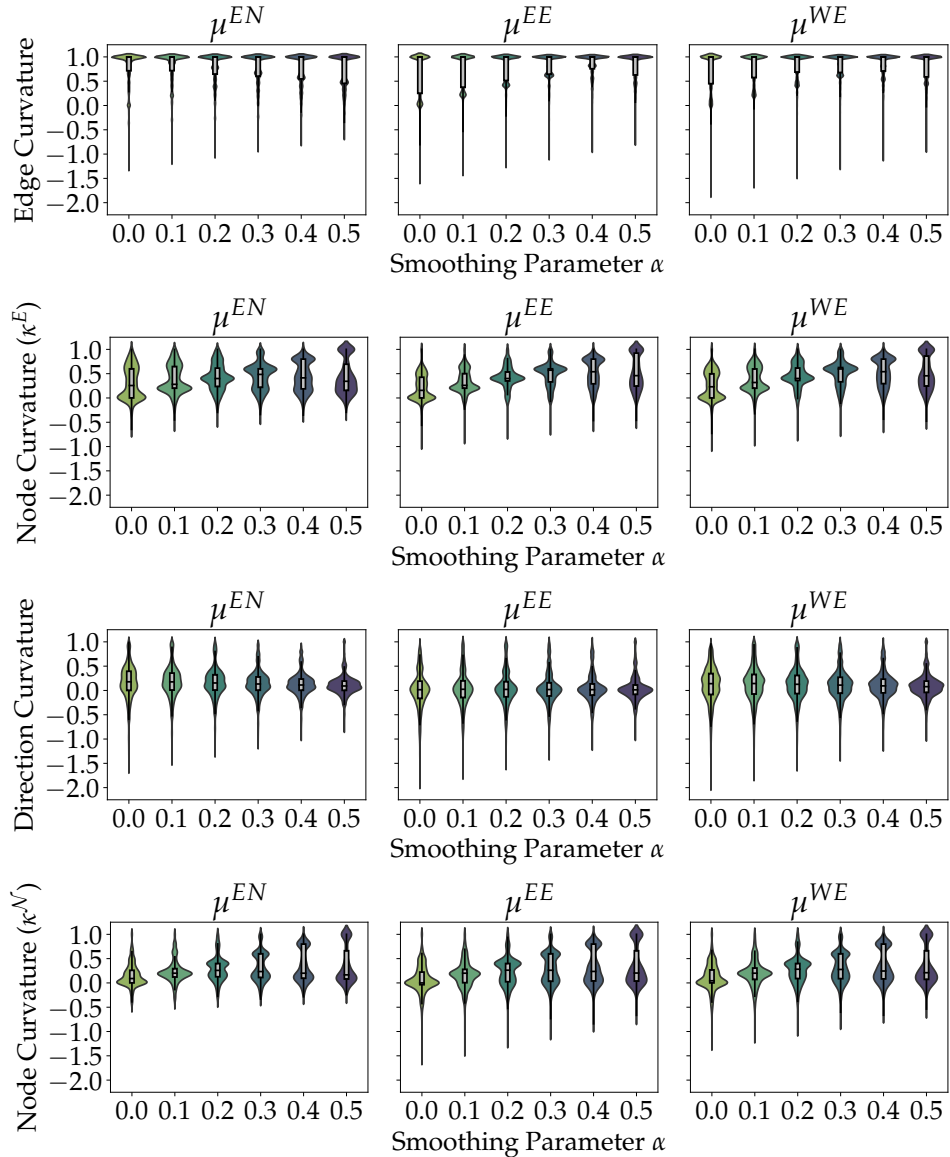


(a) Top Conferences in Machine Learning



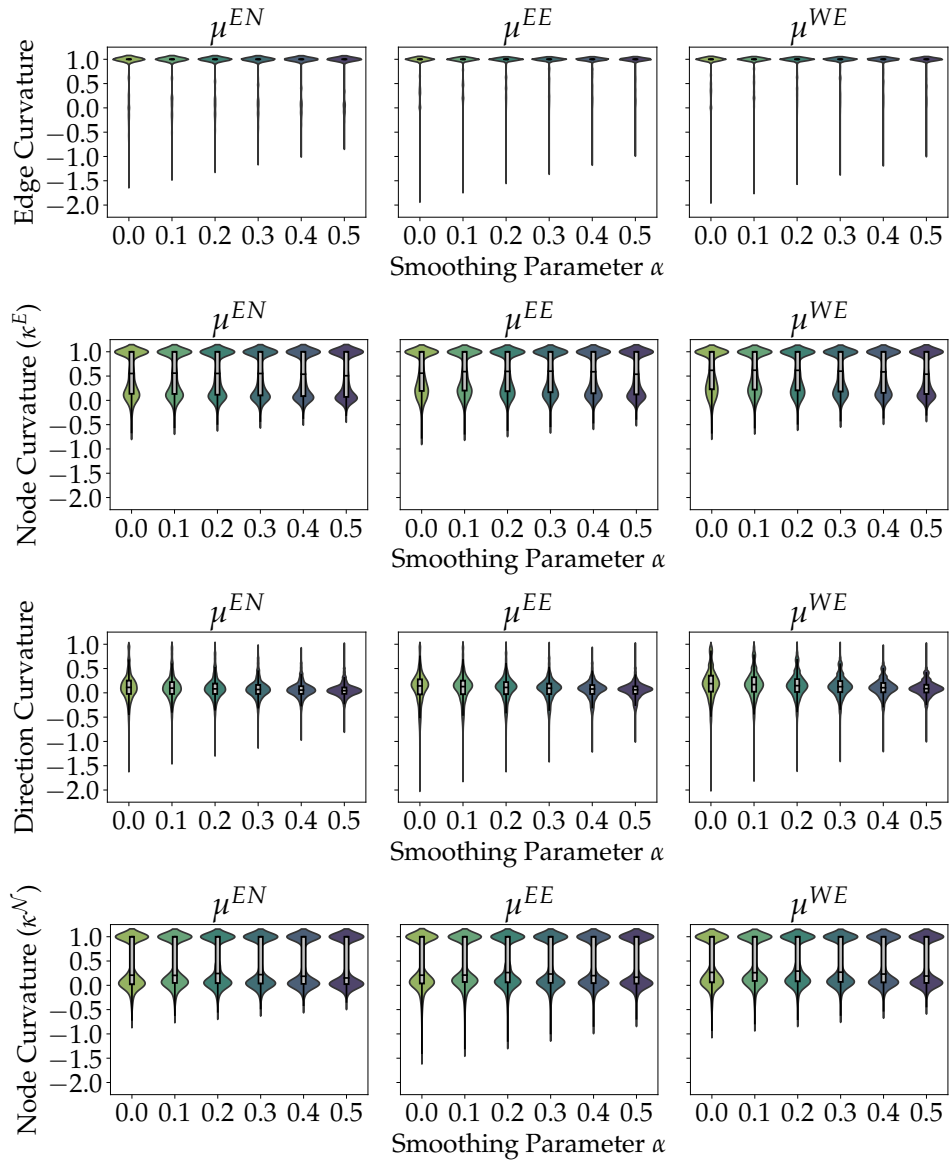
(b) Top Conferences in Theoretical Computer Science

Figure 5: ORCHID curvatures are non-redundant. We show distributions of ORCHID edge curvatures (top) and edge-averaged node curvatures (bottom) using probability measures μ^{EN} , μ^{EE} , and μ^{WE} with smoothing α , for the aggregation functions $AGGM$ (light blue) and $AGGA$ (dark blue) on dblp-v hypergraphs representing top conferences in machine learning and in theoretical computer science.



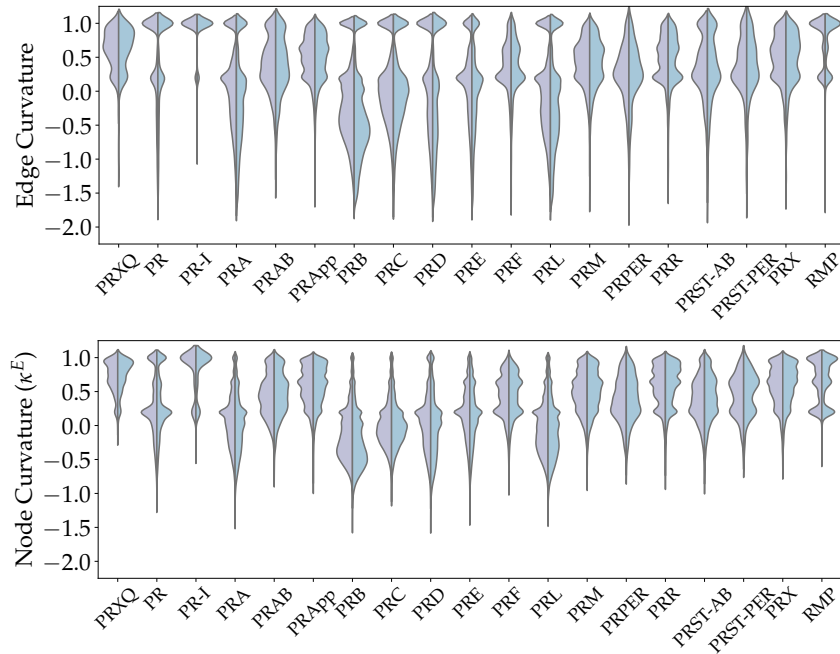
(a) ndc-pc

Figure 6: Hypergraphs with similar distributions of one curvature type may differ in their distributions of other curvature types. We show ORCHID curvatures computed using AGG_A , for all curvature types, probability measures, and $\alpha \in \{0.0, 0.1, 0.2, 0.3, 0.4, 0.5\}$. (Figure continues on next page.)

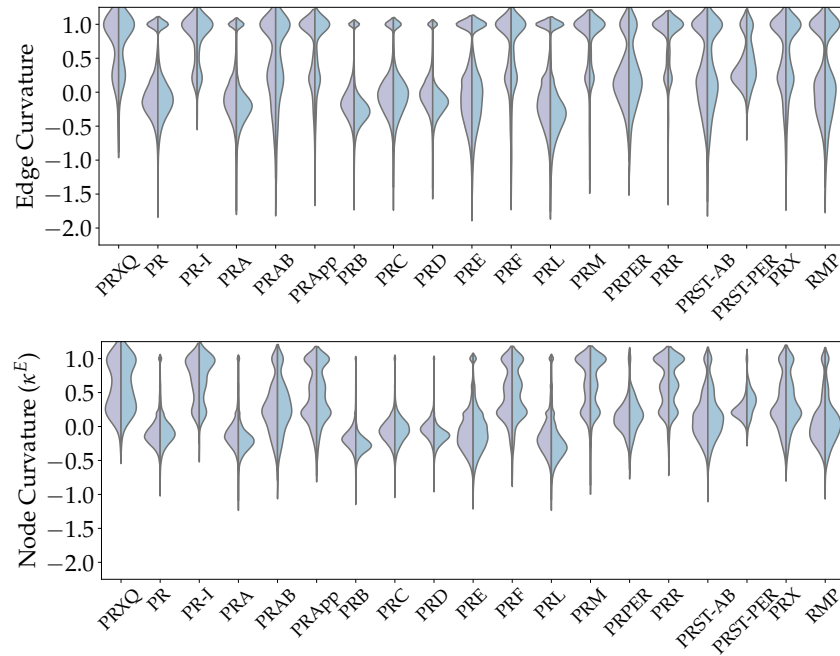


(b) ndc-ai

Figure 6: Hypergraphs with similar distributions of one curvature type may differ in their distributions of other curvature types. We show ORCHID curvatures computed using AGG_A , for all curvature types, probability measures, and $\alpha \in \{0.0, 0.1, 0.2, 0.3, 0.4, 0.5\}$. (Figure continued from previous page.)



(a) aps-av



(b) aps-cv

Figure 7: ORCHID curvature distributions within the same collection and across semantically related collections exhibit prototypical shapes, accompanied by varying types of relationships between probability measures. We show distributions of ORCHID edge curvatures (top) and edge-averaged node curvatures (bottom) computed using $\alpha = 0.1$ and AGG_A , for μ^{EE} (violet) and μ^{WE} (blue), for all hypergraphs in aps-av and aps-cv. Recall that the edges in aps-av and aps-cv as well as the nodes in aps-cv represent essentially the same set of APS papers, but in aps-av, they connect co-authors, and in aps-cv, they connect co-cited papers (edges) or are connected by citing papers (nodes).

Table 12: Top articles display varying relationships between different curvature values. We list the PRE articles that, out of all PRE articles cited at least 100 times, exhibit the most extreme curvature-related values.

	DOI	$\kappa^E(i)$	$\kappa^N(i)$	$\Delta(\kappa(i))$	$\kappa(e)$	Title
$\max \kappa^E(i)$	10.1103/PhysRevE.70.066111	0.220092	-0.006001	0.226093	0.425336	Finding community structure in very large networks
$\max \kappa^N(i)$						
$\min \kappa^E(i)$	10.1103/PhysRevE.47.851	-0.319638	-0.555431	0.235793	0	Scale-invariant motion in intermittent chaotic systems
$\min \kappa^N(i)$	10.1103/PhysRevE.48.R29	-0.241216	-0.704752	0.463536	0	Extended self-similarity in turbulent flows
$\max \Delta(\kappa(i))$	10.1103/PhysRevE.64.056101	-0.131542	-0.668266	0.536724	0.038477	Determining the density of states for classical statistical models: A random walk algorithm to produce a flat histogram
$\min \Delta(\kappa(i))$	10.1103/PhysRevE.74.016118	-0.015495	-0.191193	0.175697	-0.156824	Amorphous systems in athermal, quasistatic shear
$\max \kappa(e)$	10.1103/PhysRevE.57.610	0.129557	-0.251635	0.381192	0.610123	Topological defects and interactions in nematic emulsions
$\min \kappa(e)$	10.1103/PhysRevE.64.016706	-0.191094	-0.552908	0.361815	-0.644446	Fast Monte Carlo algorithm for site or bond percolation

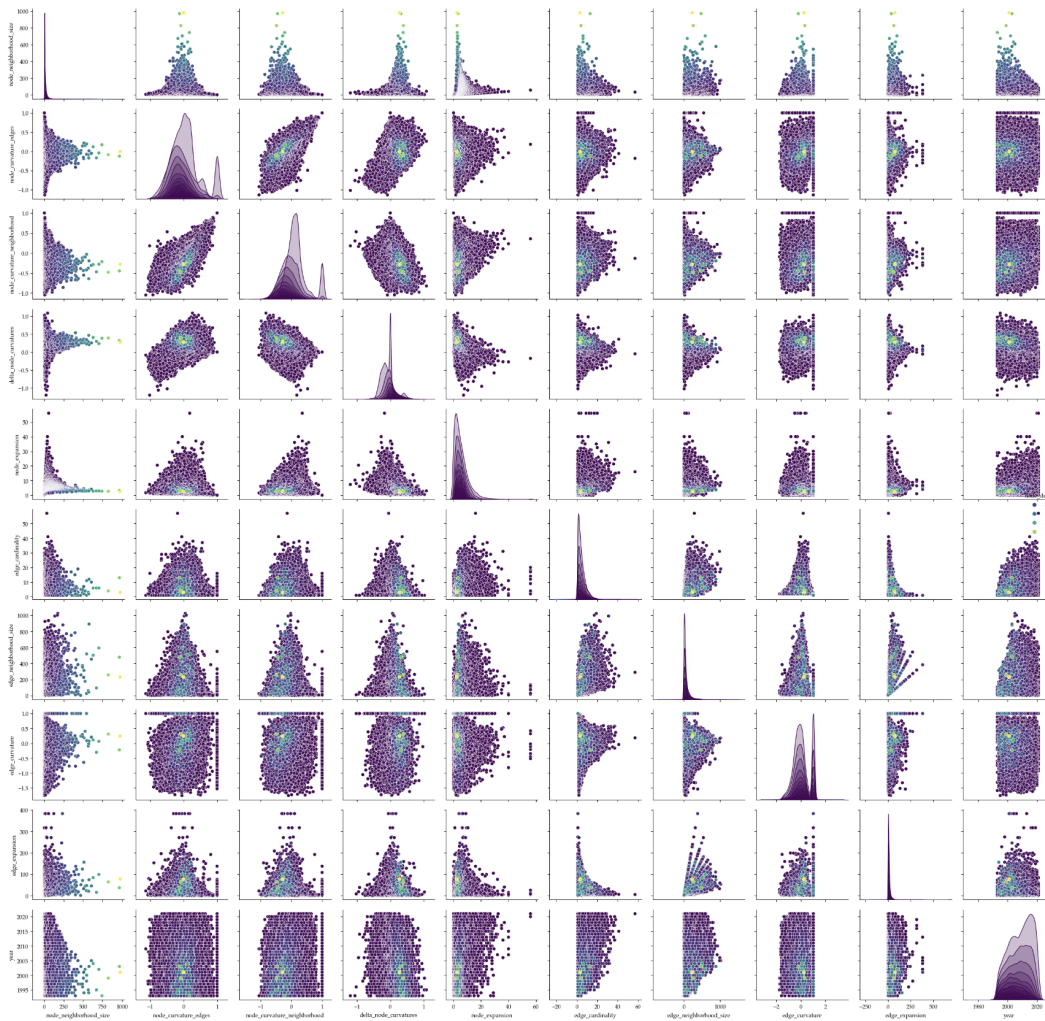


Figure 8: Highly cited articles have distinct curvature distributions. Pairwise relationships between (left-to-right, top-to-bottom) node neighborhood size, edge-averaged node curvature, direction-averaged node curvature, curvature delta, node expansion $:= \frac{\deg(i)}{|\mathcal{N}(i)|}$, edge cardinality, edge neighborhood size, edge curvature, edge expansion $:= \frac{\deg(e)}{|\mathcal{N}(e)|}$, and (as an additional metadata feature) publication year, for all PRE articles cited at least once by another PRE article, colored by node degree (number of citations within PRE), where brighter colors signal larger node degrees.

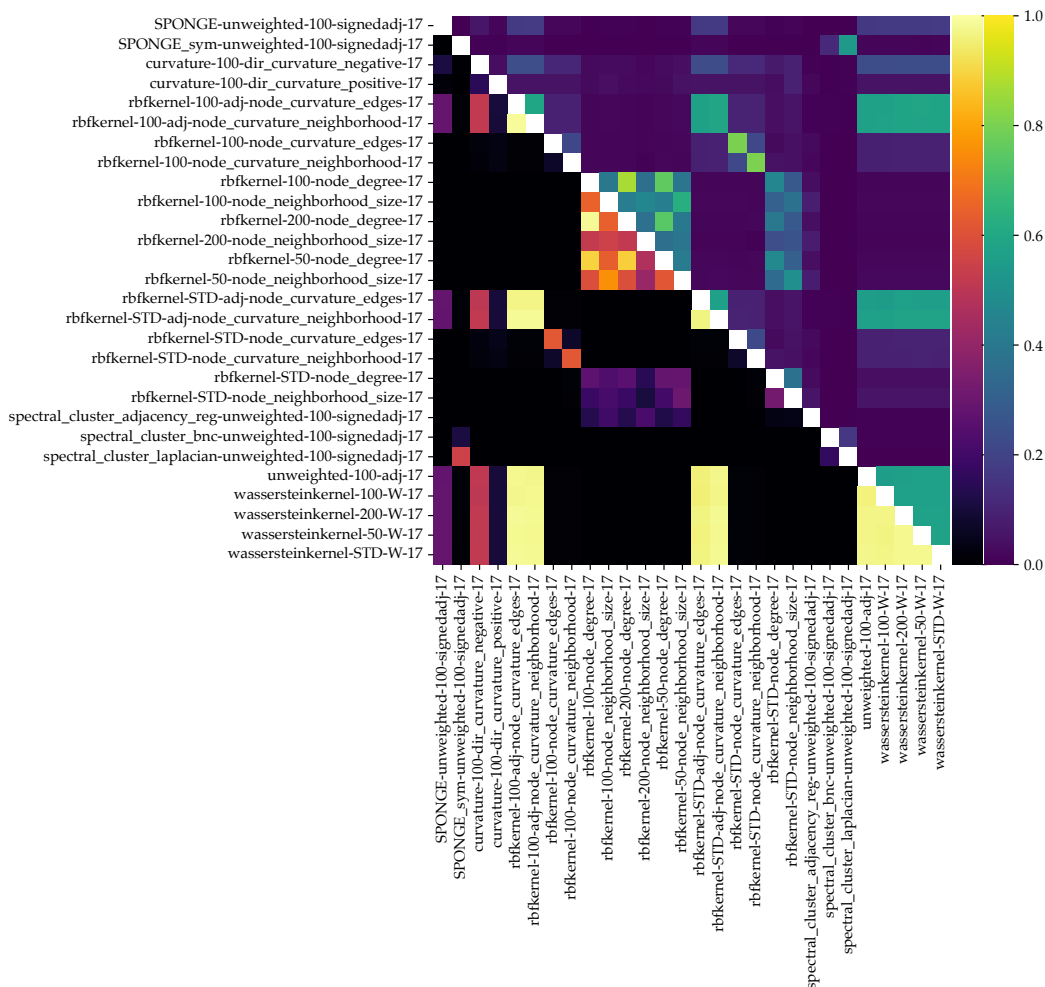


Figure 9: Node clusterings based on curvature features differ radically from clusterings based on other local features. We show the normalized mutual information (upper triangle) and the adjusted rand score (lower triangle) of node clusterings based on different method/feature combinations, computed on the citation hypergraph of PRB from the aps-cv collection, with curvatures computed using $\alpha = 0.1$, μ^{WE} , and AGGA .

Q3 Hypergraph Learning. Continuing the discussion of node clustering in hypergraphs abridged in the main paper, we again focus on the citation hypergraph corresponding to articles from Physical Review E (PRE). We experiment with a variety of features, clustering methods, and combinations thereof, including both classic and recent clustering methods, such as SPONGE (Cucuringu et al., 2019). We aim for 17 clusters, which is the number of “disciplines” present in the APS metadata (unfortunately, disciplines are only assigned to more recent articles, and hence, cannot serve as ground truth). As depicted in Fig. 9, we find that clusterings generated using curvatures as features differ radically from clusterings generated using other local features. To evaluate the semantic sensibility of our clusterings in the absence of a suitable ground truth, we leverage the metadata associated with PRE articles. In particular, we concatenate the titles of the articles grouped in each of our clusters into “documents”, and consider the set of all clusters as our “document collection”, to then identify characteristic terms for each cluster using TF-IDF feature extraction. We observe that clusterings based on ORCHID features tend to be more thematically coherent than clusterings based on other local features. As illustrated in Table 13, ORCHID features tend to separate paper titles well by topic (many frequently occurring terms are associated with only very few clusters, and the terms grouped together characterize specific subfields of the physics of collective phenomena covered by PRE), whereas clusters based on non-ORCHID features are much less topically focused.

Table 13: ORCHID features lead to node clusterings that are semantically more coherent than node clusterings derived from other local features. For two clusterings of the PRE citation hypergraph from the aps-cv collection—one a spectral clustering using the sign of directional curvatures as a feature (Table 13a), the other a clustering using an RBF kernel with node neighborhood size as a feature (Table 13b)—we show the top terms, i.e., the terms associated with each cluster that have a TF-IDF score of at least 0.1, along with their TF-IDF scores and their occurrence frequency across all clusters, in tuples of shape (term, TF-IDF score, global occurrence frequency).

(a) Feature: sign of directional ORCHID curvatures

(smectic, 0.51, 1), (liquid, 0.39, 4), (crystals, 0.22, 4), (antiferroelectric, 0.21, 1), (crystal, 0.19, 2), (phase, 0.17, 4), (chiral, 0.17, 1), (c.c., 0.15, 1), (paper, 0.15, 1), (rock, 0.15, 1), (scissors, 0.15, 1), (electric, 0.14, 1), (phases, 0.14, 2), (ray, 0.13, 1), (cyclic, 0.13, 1), (species, 0.12, 1), (field, 0.11, 3), (games, 0.1, 2)
(resetting, 0.76, 1), (stochastic, 0.32, 1), (random, 0.24, 2), (walks, 0.18, 1), (diffusion, 0.17, 2), (brownian, 0.15, 1), (processes, 0.11, 1)
(nematic, 0.66, 2), (liquid, 0.41, 4), (crystal, 0.3, 2), (colloidal, 0.26, 1), (colloids, 0.18, 1), (crystals, 0.16, 4), (particles, 0.15, 1), (interaction, 0.14, 1)
(boltzmann, 0.75, 1), (lattice, 0.51, 1), (method, 0.2, 1), (flows, 0.15, 1), (model, 0.11, 5)
(quantum, 0.58, 3), (heat, 0.38, 1), (engine, 0.34, 1), (engines, 0.27, 1), (efficiency, 0.24, 1), (performance, 0.21, 1), (power, 0.17, 1), (maximum, 0.17, 1), (otto, 0.12, 1), (carnot, 0.12, 1), (refrigerators, 0.1, 1)
(granular, 0.85, 2), (gas, 0.17, 1), (gases, 0.16, 1), (inelastic, 0.13, 1), (driven, 0.13, 1)
(chimera, 0.7, 1), (states, 0.35, 1), (oscillators, 0.33, 1), (coupled, 0.31, 2), (networks, 0.2, 3), (nonlocally, 0.13, 1), (chimeras, 0.12, 1), (coupling, 0.1, 1)
(dynamics, 0.19, 1), (model, 0.18, 5), (networks, 0.17, 3), (liquid, 0.16, 4), (diffusion, 0.13, 2), (phase, 0.13, 4), (quantum, 0.13, 3), (dimensional, 0.12, 1), (random, 0.12, 2), (flow, 0.11, 2), (systems, 0.11, 1), (plasma, 0.11, 1), (coupled, 0.1, 2), (time, 0.1, 1)
(dynamic, 0.41, 1), (ising, 0.35, 2), (phase, 0.34, 4), (oscillating, 0.34, 1), (field, 0.32, 3), (transition, 0.24, 1), (kinetic, 0.2, 1), (model, 0.2, 5), (magnetic, 0.15, 1), (nonequilibrium, 0.13, 1), (blume, 0.12, 1), (capel, 0.12, 1), (transitions, 0.11, 1)
(biaxial, 0.53, 1), (nematic, 0.5, 2), (liquid, 0.29, 4), (crystals, 0.19, 4), (phases, 0.19, 2), (bent, 0.17, 1), (phase, 0.16, 4), (molecules, 0.15, 1), (core, 0.14, 1), (simulation, 0.12, 1), (molecular, 0.1, 1), (antinematic, 0.1, 1), (mesogenic, 0.1, 1)
(passive, 0.47, 1), (scalar, 0.41, 1), (anomalous, 0.39, 1), (scaling, 0.29, 1), (advection, 0.24, 1), (turbulence, 0.22, 1), (turbulent, 0.18, 1), (advection, 0.15, 1), (loop, 0.12, 1), (anisotropy, 0.11, 1), (anisotropic, 0.11, 1), (renormalization, 0.11, 1), (vector, 0.11, 1), (field, 0.1, 3)
(quantum, 0.51, 3), (decay, 0.45, 1), (loschmidt, 0.33, 1), (echo, 0.33, 1), (fidelity, 0.25, 1), (chaotic, 0.23, 1), (semiclassical, 0.18, 1), (lyapunov, 0.13, 1), (perturbations, 0.11, 1)
(casimir, 0.69, 1), (critical, 0.37, 1), (forces, 0.27, 1), (films, 0.13, 1), (size, 0.13, 1), (force, 0.13, 1), (finite, 0.12, 1), (free, 0.11, 1), (ising, 0.11, 2), (thermodynamic, 0.1, 1), (model, 0.1, 5)
(traffic, 0.88, 1), (flow, 0.3, 2), (model, 0.13, 5), (car, 0.13, 1), (following, 0.11, 1)
(rogue, 0.62, 1), (schrodinger, 0.34, 1), (waves, 0.31, 2), (wave, 0.29, 2), (equation, 0.25, 1), (nonlinear, 0.21, 2), (solutions, 0.17, 1), (soliton, 0.12, 1), (solitons, 0.11, 1)
(cooperation, 0.6, 1), (dilemma, 0.38, 1), (prisoner, 0.34, 1), (game, 0.25, 1), (games, 0.24, 2), (evolutionary, 0.19, 1), (networks, 0.18, 3), (spatial, 0.17, 1), (social, 0.14, 1), (public, 0.12, 1), (goods, 0.1, 1)
(granular, 0.59, 2), (chains, 0.36, 1), (chain, 0.32, 1), (propagation, 0.22, 1), (waves, 0.21, 2), (nonlinear, 0.2, 2), (solitary, 0.2, 1), (wave, 0.17, 2), (pulse, 0.15, 1), (crystals, 0.14, 4), (strongly, 0.12, 1)

(b) Feature: node neighborhood size

(relation, 0.37, 1), (entropy, 0.34, 1), (differences, 0.34, 2), (production, 0.34, 1), (theorem, 0.34, 1), (work, 0.31, 2), (fluctuation, 0.29, 1), (nonequilibrium, 0.27, 2), (free, 0.27, 5), (energy, 0.27, 3)

(model, 0.25, 5), (phase, 0.23, 5), (dimensional, 0.2, 3), (dynamics, 0.18, 6), (time, 0.17, 4), (networks, 0.16, 10), (lattice, 0.15, 7), (systems, 0.15, 8), (granular, 0.13, 6), (stochastic, 0.13, 2), (random, 0.12, 6), (noise, 0.12, 1), (liquid, 0.12, 4), (nonlinear, 0.12, 2), (field, 0.12, 2), (diffusion, 0.11, 4), (quantum, 0.11, 4), (coupled, 0.11, 2), (transition, 0.11, 5), (boltzmann, 0.1, 6)

(model, 0.28, 5), (networks, 0.25, 10), (lattice, 0.22, 7), (boltzmann, 0.21, 6), (equations, 0.19, 2), (stochastic, 0.15, 2), (dynamics, 0.14, 6), (transition, 0.13, 5), (synchronization, 0.13, 3), (granular, 0.13, 6), (time, 0.13, 4), (scale, 0.13, 3), (glass, 0.13, 2), (systems, 0.12, 8), (random, 0.12, 6), (dimensional, 0.12, 3), (phase, 0.12, 5), (diffusion, 0.11, 4), (complex, 0.1, 3), (reaction, 0.1, 1), (free, 0.1, 5)

(model, 0.32, 5), (microstates, 0.27, 1), (auxiliary, 0.27, 1), (violating, 0.27, 1), (connections, 0.24, 1), (generate, 0.24, 1), (steady, 0.22, 1), (collisions, 0.22, 1), (ising, 0.2, 1), (approach, 0.2, 2), (distribution, 0.2, 1), (second, 0.2, 1), (law, 0.2, 1), (generalized, 0.2, 1), (arbitrary, 0.2, 2), (equilibrium, 0.18, 2), (synchronization, 0.18, 3), (chaos, 0.17, 1), (gases, 0.17, 2), (states, 0.17, 2), (granular, 0.15, 6), (networks, 0.13, 10)

(equation, 0.22, 4), (fokker, 0.19, 1), (planck, 0.19, 1), (hard, 0.19, 2), (fractional, 0.17, 1), (dynamics, 0.16, 6), (observable, 0.13, 1), (evolution, 0.12, 1), (characteristics, 0.12, 1), (quasistatic, 0.12, 1), (correction, 0.12, 1), (cohesion, 0.12, 1), (pair, 0.12, 1), (nearly, 0.12, 1), (ordered, 0.12, 1), (characterization, 0.12, 1), (preasymptotic, 0.12, 1), (formulas, 0.12, 1), (thermalization, 0.12, 1), (depinning, 0.12, 1), (theorems, 0.11, 1), (low, 0.11, 1), (amorphous, 0.11, 2), (intermittency, 0.11, 1), (hydrodynamics, 0.11, 1), (avalanche, 0.11, 1), (athermal, 0.11, 1), (correlation, 0.11, 2), (transport, 0.11, 1), (solution, 0.11, 1), (jammed, 0.11, 2), (propelled, 0.11, 1), (collective, 0.11, 1), (interacting, 0.11, 1), (asymptotic, 0.11, 1), (heterogeneity, 0.11, 1), (singularities, 0.11, 1), (dense, 0.1, 2), (highly, 0.1, 1), (near, 0.1, 1), (inelastic, 0.1, 1), (quantum, 0.1, 4), (fluid, 0.1, 2), (self, 0.1, 2), (shear, 0.1, 2), (rheology, 0.1, 2), (flow, 0.1, 3), (work, 0.1, 2), (liquids, 0.1, 1), (growth, 0.1, 1), (laws, 0.1, 1), (application, 0.1, 1), (disordered, 0.1, 1), (walks, 0.1, 1)

(networks, 0.38, 10), (scientific, 0.22, 1), (collaboration, 0.19, 1), (path, 0.19, 1), (ii, 0.16, 1), (density, 0.14, 2), (diffusion, 0.14, 4), (herds, 0.12, 1), (theory, 0.12, 4), (systems, 0.12, 8), (granular, 0.12, 6), (random, 0.12, 6), (schools, 0.11, 1)

(lattice, 0.27, 7), (networks, 0.26, 10), (boltzmann, 0.21, 6), (phase, 0.18, 5), (models, 0.16, 1), (structure, 0.16, 2), (method, 0.16, 4), (interactions, 0.14, 1), (self, 0.14, 2), (network, 0.13, 2), (community, 0.13, 2), (social, 0.12, 1), (free, 0.12, 5), (dimensions, 0.12, 1), (scale, 0.12, 3), (granular, 0.11, 6), (random, 0.11, 6), (systems, 0.11, 8), (motion, 0.1, 1), (graphs, 0.1, 2), (transition, 0.1, 5), (emulsions, 0.1, 1)

(networks, 0.24, 10), (glass, 0.17, 2), (transition, 0.17, 5), (lattice, 0.15, 7), (solutions, 0.14, 1), (systems, 0.14, 8), (equations, 0.13, 2), (l \hat{A} vy, 0.13, 1), (large, 0.13, 1), (external, 0.13, 1), (jammed, 0.13, 2), (flights, 0.13, 1), (correlated, 0.13, 1), (quantum, 0.12, 4), (coupled, 0.12, 2), (analysis, 0.12, 1), (force, 0.12, 1), (colloidal, 0.12, 1), (order, 0.12, 1), (packings, 0.11, 1), (synchronization, 0.11, 3), (hard, 0.11, 2), (time, 0.11, 4), (langevin, 0.11, 1), (fluctuations, 0.11, 1), (density, 0.1, 2)

(model, 0.24, 5), (dynamics, 0.22, 6), (dimensional, 0.2, 3), (phase, 0.19, 5), (liquid, 0.15, 4), (nonlinear, 0.15, 2), (systems, 0.14, 8), (field, 0.13, 2), (time, 0.12, 4), (quantum, 0.11, 4), (transition, 0.11, 5), (diffusion, 0.11, 4), (flow, 0.1, 3), (induced, 0.1, 1)

(networks, 0.41, 10), (evaluating, 0.36, 1), (uncorrelated, 0.36, 1), (generation, 0.36, 1), (finding, 0.3, 1), (structure, 0.28, 2), (community, 0.28, 2), (free, 0.26, 5), (scale, 0.26, 3), (random, 0.23, 6)

(zero, 0.55, 1), (epitome, 0.3, 1), (applied, 0.27, 1), (applications, 0.27, 1), (distributions, 0.25, 1), (stress, 0.25, 1), (arbitrary, 0.23, 2), (disorder, 0.23, 1), (degree, 0.23, 1), (temperature, 0.23, 1), (jamming, 0.23, 1), (graphs, 0.21, 2), (random, 0.17, 6)

(measurements, 0.35, 1), (hierarchical, 0.32, 1), (differences, 0.32, 2), (approach, 0.3, 2), (organization, 0.3, 2), (master, 0.3, 1), (equilibrium, 0.27, 2), (nonequilibrium, 0.25, 2), (free, 0.25, 5), (energy, 0.25, 3), (complex, 0.24, 3), (equation, 0.21, 4), (networks, 0.2, 10)

(nucleotides, 0.29, 1), (hove, 0.29, 1), (mixing, 0.26, 1), (van, 0.26, 1), (mosaic, 0.26, 1), (correlation, 0.24, 2), (dna, 0.24, 1), (patterns, 0.24, 1), (organization, 0.22, 2), (testing, 0.22, 1), (mixture, 0.22, 1), (lennard, 0.2, 1), (jones, 0.2, 1), (supercooled, 0.2, 1), (function, 0.19, 1), (coupling, 0.19, 1), (mode, 0.19, 1), (binary, 0.19, 2), (theory, 0.17, 4), (networks, 0.15, 10)

(lattice, 0.42, 7), (percolation, 0.32, 1), (boltzmann, 0.26, 6), (monte, 0.21, 1), (term, 0.21, 1), (carlo, 0.21, 1), (site, 0.19, 1), (forcing, 0.19, 1), (fast, 0.17, 1), (bond, 0.17, 1), (transitions, 0.17, 1), (algorithm, 0.17, 1), (effects, 0.16, 1), (liquid, 0.16, 4), (phase, 0.16, 5), (discrete, 0.16, 2), (network, 0.16, 2), (gas, 0.16, 2), (simulation, 0.16, 2), (nonideal, 0.16, 1), (small, 0.15, 1), (world, 0.15, 1), (scaling, 0.15, 2), (gases, 0.15, 2), (model, 0.14, 5), (method, 0.14, 4), (equation, 0.12, 4)

(viscoplastic, 0.33, 1), (dissipation, 0.29, 1), (deformation, 0.29, 1), (isotropy, 0.29, 1), (dispersion, 0.29, 1), (amorphous, 0.27, 2), (stability, 0.27, 1), (solids, 0.27, 1), (galilean, 0.27, 1), (invariance, 0.27, 1), (dynamics, 0.2, 6), (method, 0.2, 4), (lattice, 0.2, 7), (boltzmann, 0.19, 6), (theory, 0.19, 4)

(boltzmann, 0.63, 6), (lattice, 0.5, 7), (equation, 0.29, 4), (simulations, 0.21, 1), (fluid, 0.21, 2), (liquid, 0.19, 4), (gas, 0.19, 2), (binary, 0.18, 2), (method, 0.17, 4), (theory, 0.16, 4), (systems, 0.16, 8)

(plane, 0.38, 1), (flow, 0.32, 3), (dynamics, 0.26, 6), (granular, 0.24, 6), (rheophysics, 0.24, 1), (endemic, 0.21, 1), (temperatures, 0.19, 1), (equilibration, 0.19, 1), (bagnold, 0.19, 1), (inclined, 0.19, 1), (partial, 0.17, 1), (effective, 0.17, 1), (flows, 0.16, 1), (dense, 0.16, 2), (epidemic, 0.16, 1), (shear, 0.16, 2), (slow, 0.16, 1), (rheology, 0.16, 2), (discrete, 0.15, 2), (simulation, 0.15, 2), (states, 0.14, 2), (scaling, 0.14, 2), (materials, 0.14, 1), (energy, 0.14, 3), (complex, 0.13, 3), (systems, 0.12, 8), (networks, 0.11, 10)
